Title: The *Bacillus* phage SPβ and its relatives: A temperate phage model system reveals new strains, species, prophage integration loci, conserved proteins and lysogeny management components

Authors: Katharina Kohm [1], Valentina A. Floccari [2], Veronika T. Lutz [3], Birthe Nordmann [4], Carolin Mittelstädt [1], Anja Poehlein [4], Anna Dragoš [2], Fabian M. Commichau [1] and Robert Hertel [1#]

[1] FG Synthetic Microbiology, Institute for Biotechnology, BTU Cottbus-Senftenberg, 01968 Senftenberg, Germany

[2] Biotechnical Faculty, University of Ljubljana, Ljubljana, 1000, Slovenia

[3] Department of Veterinary and Animal Sciences, University of Copenhagen, Frederiksberg, 1870, Denmark

[4] Genomic and Applied Microbiology and Göttingen Genomics Laboratory, Institute of Microbiology and Genetics, Georg-August University, Göttingen, 37077, Germany

 # Corresponding author: Dr. Robert Hertel

Tel: +49 (0) 3573 85 938

Fax: +49 (0) 3573 85 809

E-Mail: Robert.Hertel@b-tu.de

Postal Adress:
BTU Cottbus-Senftenberg
Institut für Biotechnologie
FG Synthetische Mikrobiologie
Universitätsplatz 1
01968 Senftenberg

Abstract

The *Bacillus* phage SPβ has been known for about 50 years, but only a few strains are avalible. We isolated four new wild type strains of the *SPbeta* species. Phage vB_BsuS-Goe14 introduces its prophage into the *spoVK* locus, previously not observed to be used by SPβ-like phages. We could also reveal the SPβ-like phage genome replication strategy, the genome packaging mode, and the phage genome opening point. We extracted 55 SPβ-like prophages from public *Bacillus* genomes, thereby discovering three more integration loci and one additional type of integrase. The identified prophages resembled four new species clusters and three species orphans in the genus *Spbetavirus*. The determined core proteome of all SPβ-like prophages consists of 38 proteins. The integration cassette proved to be not conserved even though present in all strains. It consists of distinct integrases. Analysis of SPβ transcriptomes revealed three conserved genes, *yopQ*, *yopR*, and *yokI*, to be transcribed from a dormant prophage. While *yopQ* and *yokI* could be deleted from the prophage without activating the prophage, damaging of *yopR* led to a clear-plaque phenotype. Under the applied laboratory conditions, the *yokI* mutant showed an elevated virion release implying the YokI protein being a component of the arbitrium system.

Keywords: SPβ, φ3T, *Bacillus subtilis* 168, viral genome replication, *Spbetavirus*, arbitrium system, transcriptome, *yopQ, yopR, yokI*

Introduction

Phages or bacteriophages are viruses of bacteria and the most abundant biological entities on our planet. After infection, they take over the host metabolism and use it to reproduce. Direct reproduction is called lytic cycle, and the respective phages are called lytic phages. Temperate phages can integrate their genetic material into the bacterial genome, inactivate their lytic gene sets, and replicate with their host as a unit. This process results in a prophage and a lysogenic bacterium. A prophage can impart new features to its host through the additional genetic material and, in rare cases, even turn it into a pathogen (Kohm and Hertel, 2021).

Bacillus subtilis is a Gram-positive, rod-shaped, aerobe, spore-forming bacterium mainly found in soil (Earl *et al.*, 2008). The tryptophan auxotrophic strain *B. subtilis* 168 is capable of genetic competence (Spizizen, 1958), making it a model organism for many aspects of bacterial molecular biology (Sonenshein *et al.*, 2001). The genome of the model strains *B. subtilis* 168 was first sequenced in 1997 (Kunst *et al.*, 1997), re-sequenced in 2009 (Barbe *et al.*, 2009), and faces frequent annotation updates (Belda *et al.*, 2013; Borriss *et al.*, 2018), making it one of the best-characterised bacterial genomes. The genomic investigations revealed one integrative and conjugative element (ICEBs1) (Auchtung *et al.*, 2016), four prophage-like regions, and two prophages, known as PBSX (Seaman *et al.*, 1964) and SPβ (Brodetsky and Romig, 1965). All these alien genomic elements are non-essential for *B. subtilis* 168 and can be deleted from its genome (Westers *et al.*, 2003). *B. subtilis* is a key species of a species complex known as the *B. subtilis* clade or just Subtilis-clade (Fritze, 2004; Rooney *et al.*, 2009). It consists of closely related species like *B. subtilis*, *B. velezensis, B. amyloliquefaciens, B. licheniformis*, *B. glycinifermentas, B. vallismortis, B. atrophaeus, B. safensis, B. sonerensis, B. pumilus* (Fan *et al.*, 2017). They are mainly mesophiles and neutrophils and morphologically similar (Fritze, 2004). Members of this clade provide suitable hosts for phages initially isolated on *B. subtilis*, like φ29 (Reilly and Spizizen, 1965; Meijer *et al.*, 2001), SP-15 (Taylor and Thorne, 1963) or SPO1 (Klumpp *et al.*, 2010), and contain diverse SPβ-related prophages as recently demonstrated (Dragoš *et al.*, 2021).

Phage SPβ was independently described twice as one of two "defective" prophages of *B. subtilis* 168 (Seaman *et al.*, 1964; Hemphill and Whiteley, 1975). It resembles the *Siphoviridae* morphotype with an icosahedral head (82 to 88 nm) and a 12 nm with and 320 nm long flexible non-contractile tail, with a 36 nm wide baseplate exhibiting six equidistant, radial projections (Hemphill and Whiteley, 1975; Warner *et al.*, 1977). Its prophage is 134 kb in size and integrates into the *spsM* gene. The genome of SPβ is structured in clusters I and II containing the early phage genes and cluster III the late genes (Lazarevic *et al.*, 1999). With the discovery of *B. subtilis* CU1050, SPβ proved to be capable of lytic replication and lysogenisation (Warner *et al.*, 1977; Johnson and Grossman, 2016). Nevertheless, SPβ was discovered and described as a prophage of *B. subtilis* 168, which itself is the result of a mutagenesis experiment to gain auxotrophic mutants (Burkholder and Giles, 1947). Therefore, it is unclear if SPβ represents a wild type phage or a mutant as part of the laboratory strain *B. subtilis* 168. Many SPβ-related phage isolates are reported in the literature but were lost over the years, making SPβ and φ3T (Tucker, 1969) the last available historical isolates. Taxonomically the ICTV (International Committee on Taxonomy of Viruses) classifies the species in the genus *Spbetavirus*, which belongs to the *Siphoviridae* family (Virus Taxonomy Release 2020: https://talk.ictvonline.org/taxonomy/).

Despite over 50 years of research on SPβ, only individual aspects of its biology are understood. The "arbitrium"-system, responsible for the lysis-lysogeny decision in SPβ-related phages (Erez *et al.*, 2017; Gallego Del Sol *et al.*, 2019), and its phage-host recombination system, responsible for prophage insertion into and excision out of the hosts' chromosome (Nicolas *et al.*, 2012; Abe *et al.*, 2014, 2017, 2020), are two well-investigated exceptions. Aspects of the SPβ biology between prophage establishment and lytic replication, like lysogeny management and resolvement, or between prophage excision and particle release, are entirely dark matter and require scientific attention (Kohm and Hertel, 2021).

As temperate phages significantly impact the properties of their hosts and thereby meaningfully impact their ecology and evolution, it is of utmost importance to comprehensive explore the biology of this phage group. As a prophage of the model organism *B. subtilis* 168, SPβ is an excellent model

system. With this in mind, we aimed to use the possibilities of the genomic era to explore the genomic diversity of SPβ-related phages, extract the core components defining this phage group, and explore their potential functions if appropriate. We isolated and sequenced new wild type SPβ phages and revealed the mode of viral genome replication and packaging employed by SPβ. Through the investigation of SPβ prophages, we found new prophage insertion locations and discovered new SPβ-related viral species. The discovery of the SPβ core genes in combination with prophage transcriptomes and deletion experiments revealed new SPβ lysogeny management components.

Material and Methods

Phage isolation and generation of lysogenic strains

Bacillus subtilis Δ6 (Westers *et al.*, 2003) and *B. subtilis* TS01 (Schilling *et al.*, 2018) served as host strains. Wild type SPβ-like phages were isolated using the agar overlay plaque technique as described previously (Willms *et al.*, 2017). Agarose overlay consisted of LB medium supplemented with 0.4 % (w/v) agarose. Sterile filtered raw sewage water from the Göttingen municipal sewage plant (Göttingen, Germany, 51°33'15.4" N 9°55'06.4" E) served as a source for phage isolation. All four isolated phages were submitted to the public "German Collection of Microorganisms and Cell Cultures GmbH" (DSMZ) and thereby made avalible to the scientific community.

Lysogens were isolated from turbid plaques by picking those with a sterile toothpick and resuspending the host cells in sterile LB (10 g * L^{-1} tryptone; 5 g * L^{-1} yeast extract; 10 g *L^{-1} NaCl (Miller, 1972)). Dilutions of this suspension were spread on LB agar plate. Single colony forming units (CFU) were inoculated in 4 ml LB medium and cultured for ~ 16 h at 37 °C at vigorous shaking. Cells were removed by centrifugation 13,000 g*1 min^{-1}. The supernatant was used for agar overlay plaque assay with *B. subtilis* Δ6 or *B. subtilis* TS01 to verify the spontaneous release of viral particles from the present prophage. Observed plaques confirmed the presence of a lysogen.

Phage genome sequencing

Phages were sequenced from phage DNA and as prophages from chromosomal DNA of their lysogens. In the case of direct phage DNA sequencing, phages were first singularized via an overlay plaque assay. A single plaque was picked with a sterile toothpick and resuspended in sterile 500 µl LB. The obtained phage suspension was used to infect a 4 ml LB culture of a susceptible host at the logarithmic growth with an OD_{600} of ~ 0.8 and incubated at 37 °C at vigorous shaking until total lysis of the culture. The lysed culture was centrifugated at 5,000 g for 5 min to pellet remaining cells and cell debris. The phages in the supernatant were sterile filtered with an 0.45 µl syringe filter (Sarstedt, Nümbrecht, Germany), supplied with 5 U/ml salt active nuclease (SERVA Electrophoresis GmbH,

Heidelberg, Germany) and incubated for ~ 16 h at 8 °C to remove free nucleic acids. At the same incubation period, the phages were also precipitated by setting the suspension to 0.5 M NaCl and 10 % (w/v) polyethylene glycol (PEG) 6000 (Sigma-Aldrich, Taufkirchen, Germany). Precipitated phages were pelleted with 14,000 g for 30 min, the supernatant discarded, and the phage pellet used for phage DNA preparation with the MasterPure complete DNA and RNA purification kit (Epicentre, Madison, WI, USA).

Lysogenic bacteria were grown in a 4 ml LB medium and cultured for ~ 16 h at 37 °C at vigorous shaking, 1 ml of this culture was pelleted, and the cells were used for chromosomal DNA preparation. Phage and bacterial genomic DNA were prepared with the MasterPure complete DNA and RNA purification kit (Epicentre, Madison, WI, USA).

Illumina paired-end shotgun libraries were prepared with the NEBNext Ultra II FS DNA Library Prep (New England Biolabs GmbH, Frankfurt, Germany) for SPβ, Goe11 and Goe14 and Nextera XT DNA Sample Preparation Kit (Illumina, San Diego, CA, USA) for Goe12, Goe13 and lysogens and sequenced with the MiSeq system and reagent kit V.3 (2 x 300 bp) (Illumina, San Diego, CA, USA) and the NovaSeq system (2x 150bp) with GENEWIZ, Leipzig, Germany.

Raw reads were quality analysed with FastQC (https://www.bioinformatics.babraham.ac.uk/projects/fastqc/) and, if necessary, quality processed with Trimmomatic 0.39 (Bolger *et al.*, 2014). All obtained sequences were submitted to the SRA archive. Respective accession numbers can be found in supplementary materials 1.

Genome assembly and annotation

Phage genomes were assembled with the Unicycler v0.4.8 pipeline (Wick *et al.*, 2017) employing SPAdes version: 3.14.0 (Bankevich *et al.*, 2012) and accepted as complete when resulting in a circular replicon. The final phage genome was orientated like the SPβ c2 genome (Lazarevic *et al.*, 1999). The protein-coding genes were initially predicted and annotated with the Prokka 1.14.5 pipeline (Seemann, 2014), complemented with an InterProScan5 (Jones *et al.*, 2014) protein domain search and finally

manually curated. Individual proteins were also investigated with the web-based InterProScan version (https://www.ebi.ac.uk/interpro/).

The genome of the Goe14 lysogen was artificially constructed *in silico*. Therefore, the viral sequence reads were mapped to the genome sequence of *B. subtilis* Δ6 [NZ_CP015975] using the bowtie2 read aligner version 2.2.6 (Langmead and Salzberg, 2012) with the option –local. The created alignment was visualised with Tablet 1.17.08.17 (Milne *et al.*, 2010), and so the hybrid read, consisting of host and virus sequence, was identified (supplementary materials 2). The genome of the lysogen was created by integrating the viral genome of Goe14 into the genome of *B. subtilis* Δ6 [NZ_CP015975]. The resulting prophage integration was consistent with the prophage of *B. subtilis* BS155.

Phage packaging mechanism and packaging start point determination

Phage packaging mechanism and packaging start points were determined with the PhageTerm software package running on a Galaxy instance of the Pasteur Institute (https://galaxy.pasteur.fr). Raw Illumina reads, generated with a NEBNext Ultra II FS DNA Library Prep (New England Biolabs GmbH, Frankfurt, Germany) sequence library, were used as input.

Identification of inverted repeats in the genome fragment containing the SPβ pac-site was realized with the RNAfold Web Server (http://rna.tbi.univie.ac.at/cgi-bin/RNAWebSuite/RNAfold.cgi) using standard parameters and the DNA parameters (Gruber *et al.*, 2008). The multiple sequence alignment was realized with the Clustal Omega algorithm made available on the EMBL-EBI website (https://www.ebi.ac.uk/Tools/msa/clustalo/) (supplementary materials 11)

Extraction of SPβ-like prophages

Draft genomes of *B. subtilis* strain CU1065(Z) [NZ_JADOXU010000001], and *B. subtilis* strain DBS-15(rho11) [JADOXP010000001] were downloaded from GenBank and alight to the genome of *B. subtilis* 168 [NC_000964] with Mauve 20150226 build 10 for Windows (Darling, 2004). Contigs containing the SPβ-related prophage were identified and extracted using Artemis Release 18.1.0

(Carver *et al.*, 2011). The so obtained prophage genomes of Z and ρ11 were compared to SPβ using Mauve 20150226 build 10 for Windows (Darling, 2004).

The bioinformatic identified SPβ-related prophages by Dragoš and co-workers (Dragoš *et al.*, 2021) served as a starting point for curating and extracting new SPβ-related prophages. Derivate strains of *B. subtilis* 168 were excluded. Prophages that were known to reside in *spsM* and *kamA* were extracted from the host-genomes using Artemis Release 18.1.0 (Carver *et al.*, 2011) and, if appropriate, orientated like SPβ c2 [NC_001884] (Lazarevic *et al.*, 1999) for comparative analysis.

To identify new integration loci, genomes of the lysogens were directly compared with the genome of *B. subtilis* 168. A BLASTn comparison file was created by using makeblastdb and BLASTn version 2.10.0 (Altschul *et al.*, 1990). The comparison was visualised with ACT Release 18.1.0 (Carver *et al.*, 2011). The SPβ-like prophages were tracked and identified through their homology to SPβ specific genes. The prophage boundaries were predicted through the presence of a site-specific recombinase gene. The integration locus and the exact *attP* and *attB* sites were identified through sequence comparison of gene fragments flanking the identified prophages with an intact counterpart in *B. subtilis* 168 or closely related strains. Those were identified via BLASTn against the NCBI nr database. The *attB* sites were defined when they fit the intact template, and *attP* sites were defined as a deviating variant of the *attB* site. For integration loci, where *attP* and *attB* matched each other, the instance located close to the viral integrase was considered *attP*. All this was realised with the bioinformatical tools Artemis Release 18.1.0 (Carver *et al.*, 2011) and Mauve 20150226 build 10 for Windows (Darling, 2004).

Prophage genome re-annotation

We used the prokka pipeline 1.14.5 (Seemann, 2014) with standard parameters to re-annotate all previously identified prophages. This procedure provided uniform protein annotation for all genomes and was particularly required as some host *Bacillus* genomes had no protein annotation, like *B. velezensis* W1 [CP028375].

Spbetavirus core genome identification

Protein sequences from the re-annotated genomes were used as input for orthology detection with Proteinortho6 (Lechner *et al.*, 2011). The calculation was performed with standard parameters employing DIAMOND v0.9.29.130 (Buchfink *et al.*, 2015) for protein-protein comparison. MS Excel was used for data evaluation.

Proteins of the remnant prophage from *B. subtilis* 168 integrated into the *glnA* locus were compared to the proteins of the identified prophage in the same manner.

Transcriptome analysis

The microarray-based transcriptome data for SPβ were directly extracted from Table S2 of the study by Nicolas et. al. (Nicolas *et al.*, 2012). The RNA-seq based SPβ transcriptome data were obtained by the following procedure. Therefore, we used sequence data from Popp et. al. (Popp *et al.*, 2020) and Benda et. al. (Benda *et al.*, 2021). Raw transcriptome sequence reads were downloaded from the SRA archive using fastq-dump from sra-tools (https://github.com/ncbi/sra-tools). They were reverse complemented with the fastx_reverse_complement script from the FASTX-Toolkit (http://hannonlab.cshl.edu/fastx_toolkit/commandline.html) and mapped with to the sequence subset from *B. subtilis* 168 containing the SPβ prophage. The resulting SAM file was transformed to a tds-file and analysed with the TraV program (Dietrich *et al.*, 2014). TraV was also used to calculate nucleotide activities per kilobase of exon model per million mapped reads (NPKM). Those NPKM-values represent the normalised transcriptional activity for all protein-coding genes, which TraV could extract from the given GenBank file. Regardless of the origin of the transcription activity data, an average value for each transcription was formed and used as a demarcation line for present transcriptional activity at the dormant prophage. Genes exciding the average transcription value were considered as transcriptionally active.

Molecular cloning

If not explicitly mentioned, used molecular biological methods based on Sambrook and Russell's method collection (Sambrook and Russell, 2001). If not otherwise stated, all chemicals were dissolved in deionised water and autoclaved at 121 °C and 2 bars for 20 min. LB media was supplemented with 1.5 % (w/v) agar-agar for solid agar plates and supplemented with respective antibiotics if required. Liquid cultures were grown in 4 ml LB in glass tubes and vigorously shaken to ensure good aeration.

Escherichia coli DH10B was used as a cloning strain (Durfee *et al.*, 2008). Chemical competent cells were prepared with the $CaCl_2$ method (Sambrook and Russell, 2001). Enzymes required for cloning were obtained from ThermoFisher Scientific, Germany and used as recommended by the manufacturer.

B. subtilis strains were made competent as described by Anagnostopoulos and Spizizen (Anagnostopoulos and Spizizen, 1961) with modifications (Kohm *et al.*, 2021). *B. subtilis* mutants were created either through the transformation of the recipient stain with chromosomal DNA, a specific plasmid or PCR product. The Phusion™ High-Fidelity DNA Polymerase (2 U/µl) and HF buffer (ThermoFisher Scientific, Germany) were used as recommended by the manufacturer for PCR amplification from bacterial or viral chromosomal DNA. PCR products were analysed with a horizontal 1 % TAE agarose gel electrophoresis system (Sambrook and Russell, 2001). Specific PCR products, like the amplifications of the *yopR* gene from the SPβ clear plaque mutants, were sequenced with Microsynth SeqLab (Göttingen, Germany). Used primers, strains and plasmids are listed in supplementary materials 3, 4, and 5.

Sublancin assay

The sublancin assay verified the presence of SPβ in a lysogen. In brief, 3 µl of an overnight culture of the strains to be analysed was dropped onto a lawn of sublancin sensitive *B. subtilis* strain TS01 and incubated overnight at 37 °C. A zone of growth inhibition around the strain of interest indicated the presence of the SPβ prophage.

Results

Historical strains and new Isolates

Many SPβ-related phage isolates like IG1, IG3, IG4 (FERNANDES *et al.*, 1986) φ3T (Tucker, 1969), Z (FERNANDES *et al.*, 1986), ρ11 (Dean *et al.*, 1976), SPR (Noyer-Weidner *et al.*, 1983) and H2 (Zahler, Korman, Thomas, and Odebralski, 1987) are reported in the literature. However, only a few are sequenced and still available as an active sample. The type phage SPβ was sequenced twice as a prophage of the model organism *B. subtilis* 168 and a heat-inducible c2 mutant. The phage φ3T was sequenced during the investigation of the arbitrium system (Erez *et al.*, 2017). Recently, further historical SPβ-like isolates were sequenced through the whole genome sequencing of their lysogens. In this way, the genome of phage Z [NZ_JADOXU010000001], ρ11 [JADOXP010000001], and H2 [CP041693] were made available (Table 1).

Besides the historical phages, we isolated four new SPβ-like environmental strains named vB_BsuS_Goe11 (Goe11), vB_BsuS_Goe12 (Goe12), vB_BsuS_Goe13 (Goe13), and vB_BsuS_Goe14 (Goe14). Whole-genome sequencing of those phages revealed Goe12 representing the smallest and Goe13 the largest genome, respectively (Table 1). BLASTn based average nucleotide identity analysis with all as functional assumed SPβ-like phage genomes revealed all phages of the same species apart of H2. Phage H2 represents a distinct species closely related to SPβ (Figure 1 A and Table S1).

The new wild type isolates formed significantly larger plaques on overlay agar, indicating more efficient reproduction than the original SPβ (Figure 1 B). Phage Goe13 revealed almost clear plaques. However, it is still can able to establish lysogeny like the remaining SPβ-like phages. All in all, the new isolates present new wild type SPβ-like phages, which can serve as model systems in the investigations of SPβ-like phage biology.

Goe14 forms a new type of prophage

The genome sequences revealed Goe11 to contain an *attP* site similar to φ3T, and Goe12 and Goe13 similar to SPβ. Sequencing of Goe11 and Goe12 lysogens proved the integration of the prophages into *kamA* and *spsM* genomic loci, respectively (data not shown). Goe14 revealed an unknown *attP* site. However, as this strain successfully lysogenised *B. subtilis,* we assumed a potentially new integration locus for this phage. By searching the Goe14 raw reads for phage-host hybrids (supplementary materials 2), we could identify the *spoVK* gene of *B. subtilis* as a potential integration locus of Goe14. Like *kamA* and *spsM* (Feucht *et al.*, 2003), *spoVK* is a sporulation associate gene (Fan *et al.*, 1992; Eichenberger *et al.*, 2004). Reconstruction of the Goe14 lysogen and the BLASTn based investigation of the transition area (200 bp host plus 200 bp phage) led to the identification of a 100% identical sequence pattern in the genome of *B. subtilis* BS155 [CP029052.1]. The *B. subtilis* BS155 chromosome revealed an SPβ-like prophage integrated into the *spoVK* gene, as observed with Goe14. With both data sets in hand, we recovered the *attP* and *attB* (*attP/B*) sites of Goe14 and the BS155 prophage. The duplicated direct repeat consists of the three bases AAG, which is a rather short sequence compared to the *attP/B* site of SPβ (ACAGATAAAGCTGTAT). The minimal size explains why we were not able to identify the *attP/B* site of BS155 with a prophage prediction tool like PHASTER (Arndt *et al.*, 2016). However, the size is not unusual as the *attP/B* sites of φ3T also consist of only the five bases CCTAC (Suzuki *et al.*, 2020). In the *spoVK* gene, the AAG triplet codes for a lysine triplet. On the Goe14 genome, the *attP* site locates in the C-terminal coding region of the phage integrase, the equivalent to *sprA* from SPβ. Upon integration, the integrase gene undergoes truncation (Figure 1 C). As no *sprB* gene equivalent was observed in the Goe14 genome, one could speculate the truncation of the integrase to fulfil a regulatory function. The extended version present on the circular phage genome could be responsible for the integration and its truncated prophage form for the excision of the prophage upon reactivation for lytic replication. In such a case, the integrase gene is likely to be transcriptionally regulated and not constitutively expressed like with SPβ (Abe *et al.*, 2014).

Taken together, the genome of Goe14 reveals a third integration locus of SPβ-like phages into the chromosome of *B. subtilis* and potentially a new regulatory circuit, which controls integration and excision of the phage.

Genome replication, opening and packaging

Previous endonuclease restriction studies of SPβ genomic DNA extracted from viral particles indicated the location of the genome opening site and packaging starting point between *yonR* (BSU_21020) and *yonP* (BSU_21030) (Fink and Zahler, 1982). Analysing raw sequence reads of four SPβ-related isolates confirmed the genome-opening sites to locate between *yonR* and *yonP*. Furthermore, we precisely identify their genome opening points (Figure 2, right panel). An alignment of the first ~250 bp from all four genomes revealed a consistent starting point of the particle-packed genome for three out of four genomes. The genome opening point of Goe11 deviates. Looking at the coverage plots of Goe11, we can see that it does not have a sharp edge of the aligned reads, which is needed for genome opening point prediction (Figure 2 C, right panel). We take this as an indication of the automatic prediction to be slightly imprecise and the actual opening point to consistent with the three identified.

The raw read mapping also indicated the potential mode of genome replication and packaging employed by the SPβ-like phages. For φ3T, we can see that after the mapping peak, which represents the genome opening point, reads strongly accumulate at its left side and fade out with increasing distance from the opening point. From this observation, we can first conclude that the phage genome is packed counter-clockwise. Second, the phage genome has to be concatemeric, allowing it to fill 100 %-plus into the phage head. The observed fade out over a relatively long distance, best observed with Goe11 (Figure 2 C, left panel), indicates a head-full packaging mechanism and a circular permutation of the particle packed viral genomes. The degree of circular permutations in a viral population seems to be strain specific. No read accumulation over a significant distance was observed for SPβ, indicating almost no circular genome permutations packet into its virions. The φ3T phage reveals an evident read accumulation, and Goe11 the most pronounced. The remaining question is,

329 what size is the "plus" which results from the head-full packaging and leads to the circular
330 permutation. As this information is impossible to extract from the given sequence data, it has to be
331 experimentally explored in future.

332 SPβ-like prophage diversity and their *attB* sites

333 In times of the genomic era, many bacterial genomes are publicly available. A recent bioinformatic
334 search for SPβ-related prophages in publicly available complete *Bacillus* genomes by Dragoš and co-
335 workers revealed additional SPβ-related prophage candidates (Dragoš *et al.*, 2021). We reviewed this
336 list of potential candidates and extracted the prophage genomes of all lysogens manually. Thereby we
337 considered only prophages with a genome size of more than 120 kbp that contained a *sprA*-like
338 recombinase gene which allowed a precise determination of its boundaries. In total, 55 additional SPβ-
339 like prophages were recovered, distributed among ten host species of the Subtilis-clade (Table 1). We
340 recovered *pbuX*, *glnA*, *spoVFB* as new integration loci and several previously unknown *attP/B* sites
341 (Table 1). All genes serving as integration loci for SPβ-like phages reside at the replication termini of
342 a *Bacillus* genome (Figure 3).

343 Only the *spoVFB* gene seems to be associated with sporulation (Steil *et al.*, 2005). The gene *pbuX* is
344 involved in xanthine metabolism (Christiansen *et al.*, 1997), and *glnA* encodes the glutamine
345 synthetase (Commichau and Stülke, 2008). The data also revealed that SPβ-like phages could use
346 distinct regions of the same gene for its integration. That becomes particularly obvious with the *kamA*
347 gene, which reveals three different *attB* sites with *B. subtilis*, *B. velezensis* and *B. licheniformis*.
348 Multiple *attB* sites can also be observed with *spoVK* gene with *B. licheniformis* and *pbuX* in
349 *B. pumilus* and the others. Phages integrating into *kamA* of *B. licheniformis* reveal only two guanine
350 bases (GG) as duplication of their *attP/B* site, which is even smaller than in the case of Goe14. The
351 *glnA* locus represents the opposite extreme. Its *attP/B* sites duplicate 106 bases upon integration
352 (Table 1). It is also the only gene that remains intact after prophage integration. Interestingly, we
353 observed a prophage-like element in the genome of *B. subtilis* 168 directly associated with *glnA*. Even
354 no duplication of the 3' end of the *glnA* gene was present, a ~9 kbp region with a reduced CG content

355 till *xynP* (BSU_17570) can be observed. This region contains 11 protein-coding genes, of which five
356 showed similarities to SPβ-like proteins of the here identified prophages. The *ynzG* gene product
357 (BSU_17490) is similar to the SunI protein of SPβ (BSU_21490) with 81 % query cover and 32.35 %
358 identity, and YnaB (BSU_17500) revealed itself as an identical but shorter version of the SPβ YokH
359 (BSU_21590). These results conclude that *B. subtilis* 168 hosts two SPβ-like prophages. One still
360 functional prophage, known as SPβ and associated with the *spsM* gene and one almost degenerated
361 and associated with the *glnA* gene.

362 The genus *Spbetavirus* contains seven species

363 The availability of 64 SPβ-like genomes allows for the first time a holistic taxonomic analysis of these
364 phages. The base for this investigation was an average nucleotide identity analysis employing
365 BLASTn for pairwise comparison (Figure 4 and Table S2). Results revealed all genomes to be of the
366 *Spbetavirus* genus, which resolves into seven species clusters.

367 The largest species cluster consists of 27 strains includes the type strain SPβ. Phage genomes of this
368 cluster reveal an average nucleotide identity value between 95 and 100 %, typical for members of the
369 same species (Nordmann *et al.*, 2019; Baena Lozada *et al.*, 2020). To be precise, we have to say that
370 not each phage of this cluster revealed such a high level of identity to any other group member.
371 However, besides DSM 11031, all prophages had a counterpart within the cluster to bridge to the
372 remaining representatives. The prophage DSM 11031 had only 94 % identity to some of the
373 prophages, making it a new species per definition. Still, we keep this prophage within this group as we
374 see the possibility of new isolates appearing, which can connect this phage to the remaining in the
375 cluster. In addition, the majority of the investigated phage genomes originate from experimentally
376 unverified prophages holding the risk of a 1 % gap, dividing prophage DSM_11031 from the rest. Due
377 to the type strain SPβ within this cluster, it has already the ICTV approved species name *SPbeta.*

378 The majority of the *SPbeta* phages originate from host strains belonging to the *B. subtilis* species. The
379 only deviating host is *B. vallismortis* DSM 11031 [CP026362], in which the prophage integrates into
380 the *spoVK* locus and thus employs the same *attP/B* sites as other viral cluster representatives. The only

B. subtilis prophage not in this cluster were from *B. subtilis* ATCC 13952 [NZ_CP009748] and *B. subtilis* J-5 [NZ_CP018295], both using *pbuX* as integration locus. To find out if those deviations base on false annotated host strains, we calculated average nucleotide identity values for all host strains (Figure 5 and Table S3). Results revealed *B. vallismortis* DSM 11031 with 91 % identity to be genomically close related to *B. subtilis*. Furthermore, *B. subtilis* ATCC 13952 proved to be a *B. amyloliquefciens* and *B. subtilis* J-5 a *B. velezensis* strains due to a high degree of average nucleotide identity to the remaining strains of the respective species clusters (Figure 5 and Table S3). Thus, the results show that phages of the *SPbeta* species prefer *B. subtilis* as host-strains.

The second species cluster of the *Spbetavirus* contains 26 prophages. They are associated with phage H2 originating from *B. amyloliquefaciens* H (Zahler, Korman, Thomas, and Odebralski, 1987). For this reason, we propose this viral species be named *eta* for the Greek letter "H". All phages of that cluster associate with the host species *B. velezensis* and *B. amyloliquefaciens,* including those wrong classified *B. subtilis* strains mentioned above. Based on the genome data, *B. amyloliquefaciens* Y2 also has to be re-classified as *B. velezensis* (Figure 5).

The next smaller viral cluster is formed by phages associated with *B. licheniformis.* The observed viral examples are the biggest among the identified *Spbetavirus*. Therefore, we propose this viral species be named *magnus*, which is Latin for big.

The following viral cluster is formed by phages associated with *B. glycinifermentans* and *B. sonorensis*. With 86 % identity (Table S3), both host species are related but still distinct. Therefore, this is the first viral species to be clearly associated with two host species. We propose these viral species be named *bimanducare*, which assembles from the Latin words *bi* meaning two and *manducare* for eating.

The remaining three phages 145, KCTC_12796BP, and BA59 are associated with *B. pumilus* 145, *B. safensis* KCTC_12796BP, and *B. atrophaeus* BA59, respectively. Like their hosts, these orphans present separate species. We propose no species names for those viruses yet and shift the naming until more representatives are discovered and investigated.

For the first time, SPβ-like phages are classified taxonomically, revealing four species with several representatives within the genus *Spbetavirus* and three orphans with the potential to grow into independent new species. It is interesting to note, that the SPβ-like species narrowly associate with their host species implying a host-parasite co-evolution.

What defines an SPβ-like phage?

Having 64 genomes of SPβ-like prophages "in our hands" gave us an excellent opportunity to explore the conserved proteins and functions defining this phage group. We performed a new open reading frame (ORF) calling with all prophage genomes to create an even starting point. The newly annotated proteins we used for orthology detection. Of the 928 identified distinct SPβ-like proteins, 25 were present in all prophages, and 13 were absent in one or two viruses (Table 2 and Table S4).

Individual prophages may be incomplete, like we assume it for *B. velezensis* 10075. It reveals 96 % identity to the prophage of *B. velezensis* Bac57 but has an about 17 kb smaller genome than Bac57 (Table 1). A big part of the missing genetic information consists of a 15 kb fragment in cluster III, containing conserved homologues from BSU_21360 to BSU_21480. It includes the *blyA* gene coding the phage lysin, a crucial component for a functional prophage (supplementary materials 6). Thus, we considered orthologues as conserved, even missing in one or two prophages, as long as they are present in our functionally verified wild type isolates.

The early cluster I, presenting about 20 % of the phage genome, contains just *yokI* as a conserved protein. In the latest annotation of *B. subtilis* 168 [NC_000964.3], *yokI* codes for a putative RNase [BSU_21580]. We assume this annotation is based on the PANTHER (Protein ANalysis THrough Evolutionary Relationships) Classification System (Mi *et al.*, 2013). It was the only database we found to predict this function for YokI. However, this gene was also proposed to be the toxin of a type II toxin/antitoxin system (Van Melderen, 2010; Holberger *et al.*, 2012). Our analysis may resolve this controversy. YokI is conserved in all SPβ-like phages but not its predicted counterpart, the antitoxin YokJ, only present in 20 of the 64 prophages. Obviously, YokI is not associated with its predicted antitoxin, making it unlikely to be a toxin itself. The existence of two *yokJ* deletion mutants,

433 BKK21570 and BKE21570, further support this assumption (Koo *et al.*, 2017). We propose YokI to
434 fulfil an important function in the viral life cycle since it is conserved in all SPβ-like phages. However,
435 this function is not essential under laboratory conditions. We could successfully delete this gene for
436 the SPβ prophage without affecting its ability to generate viable particles (Figure 6 B III).

437 The most conserved proteins, 19 to be precise, are located in the late cluster III, which should contain
438 the structural genes of the phage (Table 2). This cluster also contains the *yonO* gene [BSU_21040],
439 coding for a unique DNA-dependent RNA polymerase (RNAP) observed only with SPβ (Forrest *et al.*,
440 2017), and the already mentioned *blyA* [BSU_21410] gene coding for an SPβ specific lysin (Regamey
441 and Karamata, 1998). Those genes indicate the specific RNAP as a key feature of the SPβ phage-type,
442 including specific structural components and a conserved SPβ-like lysin.

443 Early cluster II contains 18 conserved proteins (Table 2). Most of them are without functional
444 annotation. Those which have an annotation indicate their involvement in the phage genome
445 replication. This cluster's most prominent and best-investigated gene is *aimR* coding for the arbitrium
446 transcription regulator (Erez *et al.*, 2017). The AimR protein is a key component of the decision-
447 making system of SPβ-related phages, also known as the arbitrium system (Erez *et al.*, 2017). It is part
448 of the lysogeny-management system responsible for switching from lytic to lysogenic replication. Its
449 presence among the core genes confirms the lysogeny-management system to be conserved among
450 SPβ-related phages and implies some of the remaining homologs to be involved in lysogeny
451 maintenance and resolvement. However, the earlier proposed lysogeny repressor YonR (Lazarevic *et*
452 *al.*, 1999) was only conserved in 15 prophages and thus not even in all phages associated with
453 *B. subtilis*. Most important YonR was in none of the new wild type isolates, which are confirmed to
454 form prophages.

455 We also did not identify the site-specific recombinase SprA to be conserved among the SPβ-like
456 phages, even the presence of such a protein was set as an essential property during manually extraction
457 and curations of the SPβ-like prophages. This contradicting observation shows that although SPβ-like
458 phage all employ a site-specific recombinase, those are not all from the same type. In addition, the

integrase type used by the phage correlates with its insertion locus. The 44 SprA orthologues proteins were just present in phages associated with *spsM*, *kamA*, *pbuX* and *spoVFB*. The remaining 20 used two other integrases and integrated into *spoVK* and *glnA*. The phage Goe14 contains such an integrase which prefers *spoVK* for integration. As mentioned before, that protein truncates itself upon prophage integration (Figure 1 C). It shortens its proteins sequence by 131 amino acids and creates a 97 amino acids long new ORF being completely homolog to the truncated C-terminal end of the phage-encoded integrase (supplementary materials 7).

A domain search of the Goe14 integrase revealed it to be of the same organisation as the SprA integrase of SPβ but with a prolonged C-terminus with no similarity to any known structure (supplementary materials 8). We compared the protein sequence of the Goe14 integrase to all proteins of *B. subtilis* 168, including SPβ. Surprisingly we did not observe any relevant similarity to SprA of SPβ but a pronounced one to SpoIVCA with 28.0 % identity (61.3 % similar). SpoIVCA is the site-specific recombinase from the *skin* element, a degenerated prophage of *B. subtilis* 168 (Abe *et al.*, 2014).

The identified functional domains from Lzh-a42 integrase, which integrates the prophage into the *glnA* locus, were of distinct type and organisation (supplementary materials 8). Using its protein sequence as a query for a BLASTp search in the genome of *B. subtilis* 168 we could again reveal a related protein. It was the YdcL site-specific recombinase of the ICEBs1 element (Lee *et al.*, 2007). Their relation is also underlined by the relatively large direct repeats produced as *attL* and *attR* upon integration of the alien genetic element. With the here investigated SPβ-like phages, it was 106 bp of the *glnA* gene and in the case of the ICEBs1 60 bp of the *trnS-leu2* gene [BSU_tRNA_51] (Lee *et al.*, 2007). Additionally, the Lzh-a42 integrase is a tyrosine-type site-specific recombinase, while the integrases of SPβ and Goe14 are of the serine recombinase family.

These results prove the recombination unit of SPβ is a conserve core element of SPβ-like phages. Suzuki and colleagues (Suzuki *et al.*, 2020) recently demonstrated that those are artificially interchangeable between *skin*, ICEBs1 and SPβ and still result in a functional SPβ derivate (Suzuki *et*

al., 2020). Our *in silico* analysis indicate the interchangeability to be a frequent natural phenomenon. The best examples are Goe11 and Goe14. Both use different recombination units (Table 1) even they are gnomically very similar (Figure 4).

Lysogeny management components of SPβ

To determine which conserved proteins could be the prophage management components, we evaluated the data of Koo and colleagues (Koo *et al.*, 2017). To find the essential gene set, they individually addressed each gene of *B. subtilis* 168 with barcoded kanamycin (BKK) and erythromycin (BKE) deletion cassettes. This investigation also included the prophages of *B. subtilis* and thus also SPβ. Surprisingly, none of the SPβ genes was mentioned as essential, and we could recover BKK and BKE mutant numbers for all conserved SPβ genes. However, we noticed that not for all mutants barcodes were available. For instance, the *yopR* mutants have just a barcode for the erythromycin-based mutant [BKE20790] and non for the kanamycin-based mutant [BKK20790]. An opposite situation was observed for *yomS* [BSU_21240]. The *cwlP* gene [BSU_21350] is the only one not to have any barcode sequences at all, even two mutants were announced.

To determine which genes are transcribed from the dormant prophage, we analysed three independent transcriptome datasets from *B. subtilis* 168 under non-inducible conditions (Table S5). The first one from Nocolas and colleagues (Nicolas *et al.*, 2012) was generated with a microarray technique. From this study, we only used the control data set of the mitomycin C induction experiments. Of the SPβ conserved genes, five genes were transcriptionally active, *yopR*, *yopQ*, *yopP*, *aimR* and *yokI* (Table S5). The second data set from Popp and colleagues (Popp *et al.*, 2020) and the third data set from Benda and colleagues (Benda *et al.*, 2021) were up-to-date Illumina RNA-seq data sets. They were generated as control experiments from cells cultured in LB-medium at 37 °C at vigorous shaking. Their results revealed *yopR*, *yopQ* and *yokI* to be transcriptionally active (Table S5).

To find out which of the three proteins may fulfil the function of a prophage repressor, we reproduced the deletion experiments of Koo end colleagues (Koo *et al.*, 2017) on those specific genes. We successfully obtained *yopQ* and *yokI* mutants on an SPβ prophage (Figure 6 A). The *yopQ* mutants

grew well in the liquid medium. However, they revealed a translucent structure on plates during the sublancin activity assays, employed to verify the presence of the prophage (Figure 6 B). This observation implies cell lysis during the stationary phase. The *yokI* mutants revealed no noticeable difference in colony morphology but released about four times more SPβ virions into the supernatant than its ancestor strain (Figure 6 C).

We struggled to obtain mutants of the *yopR* gene, implying it to be the SPβ repressor. Potential *yopR* prophage mutants appeared about two days after transformation in low numbers, and their genotype could not be confirmed. Just recently and independent from our investigation, Brady and colleagues (Brady *et al.*, 2021) experienced the same struggles during their *yopR* deletion attempts. Indeed, their results revealed YopR as the master repressor of the SPβ prophage (Brady *et al.*, 2021). Our concept to prove the hypothesis of YopR being the SPβ repressor was to isolate clear-plaque mutants and investigate their genome. We isolated six of these mutants cpm1 to cpm6 from the supernatant of *B. subtilis* 168 and verified their genomes for consistency via PCR. Two of six might have faced deletions in their early operons (supplementary materials 9). Such deletions were reported in the literature for earlier identified clear-plaque mutants of SPβ (Spancake and Hemphill, 1985). The cmp2 mutant with a potentially complete genome was whole-genome sequenced with Illumina technology. Using the obtained reads for single nucleotide polymorphisms (SNPs) analysis, a deletion of 16 bp became evident in the *yopR* gene and a subsequent frameshift truncating the coding region. Next, we PCR amplified, and Sanger sequenced the *yopR* genes of the remaining clear-plaque mutants cmp3, 5 and 6 with a potentially complete genome. We observed one deleted base and one point-mutation in cpm6, which likewise in cpm2 lead to a frameshift in *yopR* and truncation of the gene. In both cpm3 and cpm5, we observed deletions of the entire intergenic region of 23 bp between *yopQ* and *yopR* (Figure 7).

All observed mutations affected the 325 amino acids (aa) long YopR protein. The observed deletion of the entire *yopQ* and *yopR* intergenic region removed the ribosome binding site of *yopR* and thereby likely abolished its translation. To find out the impact of the remaining mutations, we scanned YopR

537 for the presence of known functional domains. Using InterProScan5 we could identify a predicted
538 DNA breaking-re-joining catalytic core between 12 to 218 aa. Interestingly, only the 16 bp deletion of
539 cpm2 affected the last six C-terminal amino acids of the predicted domain. The point-mutation of
540 cpm6 was far behind at amino acid 273. To test whether these *yopR* mutations are responsible for the
541 observed clear-plaque phenotypes, we created a host strain with an artificially expressed YopR.
542 Therefore, we fused *yopR* with the constitutively active P_{alf4} promoter and introduced it into the *amyE*
543 locus of the *B. subtilis* TS01 chromosome. Employing the so created strain as host, clear-plaque
544 mutants cpm2 and cpm6 lost their lytic phenotype. They could not form plaques anymore
545 (supplementary materials 10). Consequently, our results are in good agreement with the observations
546 by Brady and colleagues (Brady *et al.*, 2021) and confirm YopR to be the prophage repressor of SPβ.
547

Discussion

Genome replication and packaging

Our investigation revealed SPβ-like phages to replicate their genomes in a concatemeric way and pack their genomic DNA via the head-full mechanism into their proheads. Such a packaging system is known from the *Escherichia virus* P1. The concatemeric viral genome is pumped into its prohead until it is full. This triggers an unspecific cut of the DNA and the release of the translocase machinery, which still holds the genome. An association with a new prohead initiates its filling with the remaining viral genomic material (Calendar, 2006).

SPβ presents itself as not very efficient in this type of genome packaging. Its apparent inability to continuously package its genome concatemer may be the reason for the relatively low replication rate (Figure 2 A). Restarting genome translocation at the pac-site after each 100 %-plus filled phage head would be an enormous waste, as it would leave a < 100 % fragment with each 100 %-plus filled phage head. Even if the left behind fragments were sufficient to ensure phage reproduction, one way or another, they still would be doomed to degeneration due to the missing pac-site, which was packed as the "plus" with the preceding filling. A phage like Goe11, which is much more successful in its reproduction judging by its plaque size (Figure 1 B), could draw its advantage from the more efficient use of its genome concatemer. If we hypothetically assume the entire reproductive process of SPβ and Goe11 to be the same, except for the genome packaging, Goe11 would generate about twice as much viable offspring as SPβ just by the continuous use of the genome concatemer. This efficient use of Goe11's genome concatemer is evident in the sequence coverage plot from its particle-packaged genomic DNA (Figure 2 C). To prove this hypothesis, one could replace the genome packaging components of SPβ with those of Goe11 and investigate the plaques and offspring numbers of the so produced hybrids. Before we can do so, we first need to identify and experimentally verify the genome packaging machinery of SPβ.

All in all, these data lead to the conclusion that SPβ-like phages pack their genomes with a head-full mechanism placing 100 %-plus genome per virion. The question of what the "plus" could be, cannot

be precisely answered from the available data. The frequently observe ~250 bp block after the opening point unlikely represents the genome overhang (Figures 2, right panel). It is precise and equal in size with all investigated isolates, even though the isolates reveal distinct genome sizes and thus hold the potential to pump overhang fragments of different sizes into their viral heads. We can speculate that the 250 bp fragment is associated with a very likely conserved translocation machinery and contains the pac-site sequence pattern. All packaging start points were the same for the investigated phages (supplementary materials 11).

The Goe14 mapping reveals a focused read accumulation of about 2 kbp following the ~250 bp peak (Figure 2 D). It represents 1.6 % of the whole genome and could be thought of as the "plus" overhang. The *Bacillus* phage SPP1, a smaller lytic *Syphoviridae* type of phage, also employ pac-sites and a head-full genome packaging mechanism (Calendar, 2006). With 1.4 kb it reveals similar terminal redundancy with the particle packed genomic DNA (Camacho *et al.*, 2003). However, for SPβ-like phages, this assumption has to be experimentally verified in the future. The observed sequence accumulation of ~2 kbp was only observed with Goe14, and its proportions are not balanced to the average coverage. It should only be twice as high as the rest of the coverage if the observed accumulation originates from the above-average initiation of genome translocation at the pac-site and the 100 %-plus head-full mechanism. However, here it is significantly higher (Figure 2 D).

Expansion of the genus *Spbetavirus* and their prophages

Isolation of new SPβ-like viruses, particularly Goe14, brought us on the track of new prophages. Their isolation revealed a whole new diversity of SPβ-related phages. For the first time, new species of the genus *Spbetavirus* were identified, strongly associated with their host genus.

We could identify five more SPβ prophage integration loci, of which *spoVK* is also actively used in derivates of *B. subtilis* 168, and *glnA* at least was used in the past by a potentially related SPβ derivate. It remains unclear if the other three integration loci, present in *B. subtilis*, are actively targeted for prophage integration. The only two potential *B. subtilis* lysogens using *pbuX* for prophage integration revealed themselves to be of a distinct bacterial species (Table 1). However, the phage H2 is known to

replicate and lysogenize *B. subtilis* CU1050, an SPβ free derivate of 168 (Zahler, Korman, Thomas, Fink, *et al.*, 1987). That observation suggests the possibility of *pbuX* as an integration locus in *B. subtilis*. Ultimately, this question can only be clarified by experimental studies.

From φ3T and SPβ, it is known that *spsM* and *kamA* are re-established during sporulation. How it appears with the here identified new integration loci is to be investigated. However, the *spoVFB* gene from *B. weihenstephanensis* KBAB4, which is disrupted by a prophage-like element, is re-established in the mother cell during spore formation to ensure dipicolinic acid synthetase (Abe *et al.*, 2013). During sporulation of *Geobacillus thermoglucosidasius* C56-YS93 a similar gene reestablishment and excision of a prophage-like element was observed with the *spoVR* gene (Abe *et al.*, 2013). Its gene product is required for spore cortex formation (Beall and Moran, 1994).

It cannot be answered at this point if there are more potential integration loci for SPβ-like phages. However, this is likely to be the case since other sporulation-related genes like *cotJC*, *gerE*, *yaaH* and *yhbH* are frequently used for phage or transposon related integrations (Abe *et al.*, 2013). Although, the mentioned examples were observed in bacterial species, not of the Subtilis-clade. Still, *spoVFB* was first observed as integration locus of the prophage-like element *vfbin* in *B. weihenstephanensis* KBAB4 (Abe *et al.*, 2013) and now revealed itself as an integration loci of a *Spbetavirus* species (Table 1). The fact that SPβ-like phage can interchange their recombination units makes us expect further diversity.

BLASTn based prophage predictions were used as a starting point for the investigation of SPβ prophage diversity. The genome of the type-strain SPβ served as a query. Thus, it is likely that just very related prophages were identified in closely related host strains (Figure 4 and 5). Most successfully extracted SPβ-like prophages originated from *B. subtilis* genomes and genomes of related *B. velezensis* and *B. amyloliquefaciens* strains. Only a few prophages came from more distinct bacterial strains. Phages on the genus border with slightly over 70 % average nucleotide identity to the remaining isolates came from *B. safensis* and *B. pumilus* (Figure 4). If repeating the prophage search with those unique phage genomes as a new query, new and more diverse *Spbetavirus* members could

626 be identified. Each round of further repetitions could even reveal the presence of SPβ-like phages
627 ahead the Subtilis-clade. However, as further search attempts would base on experimentally not as
628 functionally verified prophages, the resulting error multiplication can hardly be estimated. Thus, it is
629 better to start after prophage 145 from *B. pumilus* and KCTC_12796BP from *B. safensis* are verified
630 functional.

631 ## Multiple lysogenisation

632 Having so many phages associated with one host species like *B. subtilis,* leads to the question of how
633 many phages can simultaneously lysogenise one host. For SPβ and φ3T it is known they can
634 lysogenize the same host (Warner *et al.*, 1977). To our surprise, we frequently observed multiple
635 fragmented SPβ-like phages in one strain. For example, *B. velezensis* DKU_NT_04 [NZ_CP026533]
636 has rudiments of prophages in three of six insertion sites. An approximately 19 kbp fragment sits in
637 *spsM*, an approximately 262 kbp fragment sits in *glnA*, and a not further defined fragment in *pbuX*.
638 This strain suggests that multiple lysogenization beyond two phages may be possible. However, we
639 never observed more than one complete SPβ-like phage in the same host strain. One can only
640 speculate about the reasons. It is conceivable that phages from the same genus are simply too similar
641 to persist in the same host. Their similar genomic organisation and high sequence homology make
642 recombination of the prophages likely. That can lead to the degeneration of both involved entities or to
643 the formation of hybrids.

644 A possible indication for the degenerative recombination hypothesis is provided by the SPβ-like
645 prophages of *B. velezensis* SGAir0473. Here, we identified a prophage in both the *spoVK* and *spsM*
646 genes. Both seem to be fragmented. The prophage in *spoVK* is too large for an SPβ-like phage with the
647 size of ~ 205 kbp, and the prophage in the *spsM* gene is too tiny with ~ 30 kbp. However, the total size
648 of ~ 235 kb is about the size of two intact representatives. This example implies that the simultaneous
649 presence of two SPβ-like phages represents an unstable structure. Dragoš and colleagues were able to
650 observe the formation of possible hybrid phages and even verified them as stable viral entities (Dragoš
651 *et al.*, 2021). However, we also observed assembly artefacts during an automated genome assembly of

an SPβ and φ3T double lysogenic strain (unpublished data). Suppose the focus of such a genome assembly is not on the phages. In that case, this circumstance can easily be overlooked and lead to artificial genomes.

Finally, although the genomic study of diverse lysogens did not reveal any unambiguous double lysogens, we can suggest that this phenomenon is not limited to SPβ and φ3T. It may even have a biological function, such as creating new phage types (Dragoš *et al.*, 2021). It remains an exciting question which factors allow such a double lysogen and which role the phage repressor plays since a superinfection of the same phage in a lysogen is not possible.

SPβ core genes and its lysogeny management system

The identified conserved SPβ proteins are mainly without functional annotation. But even so, they can help to check new isolates for their relationship to SPβ if the nucleotide sequence differs significantly. Aligning the core genome to existing SPβ prophage transcriptomes proved to be a valid strategy for the identification of the SPβ lysogeny management components. This strategy is particularly interesting for other bigger prophages like SPβ, which bring several accessory genes relevant for the host and actively transcribed from the dormant prophage (Hemphill *et al.*, 1980; Dragoš *et al.*, 2020) (Table S5).

YopR is not the first protein proposed to be the prophage repressor of SPβ (Brady *et al.*, 2021). Earlier, the YonR was proposed to be the lysogenic repressor of SPβ due to its similarity to the lysogenic repressor Xre for lysogeny maintenance of PBSX and YqaE of the *skin* element (Lazarevic *et al.*, 1999). The d-protein (YomJ) also conveyed resistance against SPβ and closely related phage strains if expressed ectopically from a plasmid (McLaughlin *et al.*, 1986). However, neither *yonR* nor *yomJ* are conserved (Table 2), and both could be individually deleted from the prophage genome without activating the prophage (Koo *et al.*, 2017). However, genomic investigation of our clear plaque mutants confirmed YopR as essential for prophage establishment. Combining our results, we can even extract more knowledge about YopR. This protein has a "DNA breaking- re-joining enzymatic core" which Brady and colleagues propose as essential for the function of YopR as a

repressor (Brady *et al.*, 2021). In fact, the two clear-plaque mutants described by the group had their mutation in this particular region. The mutations of the clear-plaque mutants we identified lie at the end or behind the predicted domain (Figure 7). Particularly cpm6 proves YopR to contain new, previously unknown domains to explore.

Besides *yopR* there were two more conserved genes transcribed from the prophage. We could successfully delete both genes without induction of the prophage. The translucent cells of the *yopQ* mutants and the significantly increased spontaneous release of viable virions of the *yokI* mutants imply both proteins to be involved in the lysogeny management system of SPβ (Figure 6). The phenotype of the *yopQ* mutants does not directly allow this conclusion, but since this gene forms an operon with *yopR* and is thus transcribed together with it, we assume its involvement in lysogeny management. The phenotype of the *yokI* mutant is obvious. In Figure 8 we present our hypothesis about how YokI might be connected with the lysogeny management system of SPβ.

The arbitrium system consists of AimR, a transcription activator of the non-coding small RNA (ncRNA) AimX, and a quorum-sensing signal peptide AimP. When AimP is processed and re-imported into the cytosol, it interacts with the AimR dimer. Subsequently, this complex experiences a conformational change, dissociates from the aimX promoter, and reduces *aimX* transcription (Erez *et al.*, 2017). Brady and colleagues showed that *aimR* mutants mainly prefer lysogeny and *aimP* mutants the lytic route (Brady *et al.*, 2021). Thus, *aimX* transcription is reduced without AimR and increased without AimP. The AimX ncRNA may modulate the function of YopR and make it more slippery or tight. However, the arbitrium system is not essential for lysogeny establishment or resolvement but rather fine-tunes the system (Erez *et al.*, 2017; Otte *et al.*, 2020; Aframian *et al.*, 2021; Brady *et al.*, 2021). The question not asked before is what happens with the ncRNA AimX itself. As a strongly transcribed ncRNA it needs to have an equilibrium mechanism. Something which ensures this ncRNA does not accumulate, like an RNase keeping it in balance. YokI is the perfect candidate. It is conserved in the *Spbetavirus*, transcribed from the inactive prophage, and contains a predicted RNase domain. The increased amount of virus particles released into the supernatant of *yokI* mutants could be

704 explained by the accumulation of AimX. In such a case, it would no longer be counterbalanced and
705 accumulate like in the AimP mutant and push the system to lysis (Figur 8). This hypothesis is also
706 supported by historical data where lost fragments between *sprA* (*yokA*) and *sunI* (*yolF*), including
707 *yokI*, were associated with unstable lysogeny (Spancake and Hemphill, 1985).

708 To explore the *yokI* hypothesis and many other aspects of SPβ revealed during this work, we will go
709 ahead of the genomic perspective and devote ourselves to specific experiments to further unravel the
710 mysteries of SPβ.

711 Data Availability

712 Phage genome sequence data used for the presented investigation were either obtained from SRA and
713 GenBank repositories or created during this investigation and subsequently submitted to the public
714 SRA and GenBank repositories. The respective accession numbers can be found in Table 1 and in
715 supplementary materials 1.

716 Supplementary data

717 Supplementary data are available at bioRxiv online.

718 Funding

719 This work was supported by Volkswagen Foundation [Re. 94045] and the Max Buchner Research
720 Foundation [Re. 3799]. A.D. and V.A.F. were supported by Slovenian Research Agency [N1-0177].

721 Conflict of Interest Disclosure

722 The author declares no conflict of interest.

723 Acknowledgement

724 This work was also supported by the Georg-August University of Göttingen and the Brandenburg
725 Technische Universität Cottbus-Senftenberg. We thank all FG Synthetic Microbiology group members
726 for stimulating discussions and suggestions.

Bibliography

Abe, K., Kawano, Y., Iwamoto, K., Arai, K., Maruyama, Y., Eichenberger, P., and Sato, T. (2014) Developmentally-Regulated Excision of the SPβ Prophage Reconstitutes a Gene Required for Spore Envelope Maturation in *Bacillus subtilis*. *PLoS Genet* **10**: e1004636.

Abe, K., Takahashi, T., and Sato, T. (2020) Extreme C-terminal element of SprA serine integrase is a potential component of the "molecular toggle switch" which controls the recombination and its directionality. *Mol Microbiol* 1–12.

Abe, K., Takamatsu, T., and Sato, T. (2017) Mechanism of bacterial gene rearrangement: SprA-catalyzed precise DNA recombination and its directionality control by SprB ensure the gene rearrangement and stable expression of *spsM* during sporulation in Bacillus subtilis. *Nucleic Acids Res* **45**: 6669–6683.

Abe, K., Yoshinari, A., Aoyagi, T., Hirota, Y., Iwamoto, K., and Sato, T. (2013) Regulated DNA rearrangement during sporulation in *Bacillus weihenstephanensis* KBAB4. *Mol Microbiol* **90**: 415–27.

Aframian, N., Bendori, S.O., Guler, P., Hen, S., Stokar-, A., Msaeed, K., et al. (2021) Dormant phages communicate to control exit from lysogeny. *bioRxiv*.

Altschul, S.F., Gish, W., Miller, W., Myers, E.W., and Lipman, D.J. (1990) Basic local alignment search tool. *J Mol Biol* **215**: 403–10.

Anagnostopoulos, C. and Spizizen, J. (1961) REQUIREMENTS FOR TRANSFORMATION IN BACILLUS SUBTILIS. *J Bacteriol* **81**: 741–6.

Arndt, D., Grant, J.R., Marcu, A., Sajed, T., Pon, A., Liang, Y., and Wishart, D.S. (2016) PHASTER: a better, faster version of the PHAST phage search tool. *Nucleic Acids Res* **44**: W16-21.

Auchtung, J.M., Aleksanyan, N., Bulku, A., and Berkmen, M.B. (2016) Biology of ICE Bs1 , an integrative and conjugative element in *Bacillus subtilis*. *Plasmid* **86**: 14–25.

Baena Lozada, L.P., Hoppert, M., and Hertel, R. (2020) Phage vB_BmeM-Goe8 infecting Bacillus megaterium DSM319. *Arch Virol* **165**: 515–517.

Bankevich, A., Nurk, S., Antipov, D., Gurevich, A.A., Dvorkin, M., Kulikov, A.S., et al. (2012) SPAdes: A New Genome Assembly Algorithm and Its Applications to Single-Cell Sequencing. *J Comput Biol* **19**: 455–477.

Barbe, V., Cruveiller, S., Kunst, F., Lenoble, P., Meurice, G., Sekowska, A., et al. (2009) From a consortium sequence to a unified sequence: the *Bacillus subtilis* 168 reference genome a decade later. *Microbiology* **155**: 1758–75.

Beall, B. and Moran, C.P. (1994) Cloning and characterization of *spoVR*, a gene from *Bacillus subtilis* involved in spore cortex formation. *J Bacteriol* **176**: 2003–12.

Belda, E., Sekowska, A., Le Fèvre, F., Morgat, A., Mornico, D., Ouzounis, C., et al. (2013) An updated metabolic view of the *Bacillus subtilis* 168 genome. *Microbiology* **159**: 757–70.

Benda, M., Woelfel, S., Faßhauer, P., Gunka, K., Klumpp, S., Poehlein, A., et al. (2021) Quasi-essentiality of RNase Y in *Bacillus subtilis* is caused by its critical role in the control of mRNA homeostasis. *Nucleic Acids Res* **49**: 7088–7102.

Bolger, A.M., Lohse, M., and Usadel, B. (2014) Trimmomatic: a flexible trimmer for Illumina sequence data. *Bioinformatics* **30**: 2114–20.

768 Borriss, R., Danchin, A., Harwood, C.R., Médigue, C., Rocha, E.P.C., Sekowska, A., and Vallenet, D.
769 (2018) *Bacillus subtilis*, the model Gram-positive bacterium: 20 years of annotation refinement.
770 *Microb Biotechnol* **11**: 3–17.

771 Brady, A., Quiles-Puchalt, N., Gallego del Sol, F., Zamora-Caballero, S., Felipe-Ruíz, A., Val-Calvo,
772 J., et al. (2021) The arbitrium system controls prophage induction. *Curr Biol* 1–9.

773 Brodetsky, A.M. and Romig, W.R. (1965) Characterization of *Bacillus subtilis* Bacteriophages. *J*
774 *Bacteriol* **90**: 1655–1663.

775 Buchfink, B., Xie, C., and Huson, D.H. (2015) Fast and sensitive protein alignment using DIAMOND.
776 *Nat Methods* **12**: 59–60.

777 Burkholder, P.R. and Giles, N.H. (1947) INDUCED BIOCHEMICAL MUTATIONS IN BACILLUS
778 SUBTILIS. *Am J Bot* **34**: 345–348.

779 Calendar, R. (2006) The bacteriophages, Oxford University Press.

780 Camacho, A.G., Gual, A., Lurz, R., Tavares, P., and Alonso, J.C. (2003) *Bacillus subtilis*
781 bacteriophage SPP1 DNA packaging motor requires terminase and portal proteins. *J Biol Chem*
782 **278**: 23251–9.

783 Carver, T., Harris, S.R., Berriman, M., Parkhill, J., and McQuillan, J.A. (2011) Artemis: An integrated
784 platform for visualisation and analysis of high-throughput sequence-based experimental data.
785 *Bioinformatics* **28**: 464.

786 Christiansen, L.C., Schou, S., Nygaard, P., and Saxild, H.H. (1997) Xanthine metabolism in *Bacillus*
787 *subtilis*: characterization of the *xpt-pbuX* operon and evidence for purine- and nitrogen-controlled
788 expression of genes involved in xanthine salvage and catabolism. *J Bacteriol* **179**: 2540–50.

789 Commichau, F.M. and Stülke, J. (2008) Trigger enzymes: bifunctional proteins active in metabolism
790 and in controlling gene expression. *Mol Microbiol* **67**: 692–702.

791 Darling, A.C.E. (2004) Mauve: Multiple Alignment of Conserved Genomic Sequence With
792 Rearrangements. *Genome Res* **14**: 1394–1403.

793 Dean, D.H., Orrego, J.C., Hutchison, K.W., and Halvorson, H.O. (1976) New Temperate
794 Bacteriophage for *Bacillus subtilis*, ρ11. *J Virol* **20**: 509–519.

795 Dietrich, S., Wiegand, S., and Liesegang, H. (2014) TraV: A Genome Context Sensitive
796 Transcriptome Browser. *PLoS One* **9**: e93677.

797 Dragoš, A., Andersen, A.J.C., Lozano-Andrade, C.N., Kempen, P.J., Kovács, Á.T., and Strube, M.L.
798 (2020) Phages weaponize their bacteria with biosynthetic gene clusters. *bioRxiv*.

799 Dragoš, A., Priyadarshini, B., Hasan, Z., Strube, M.L., Kempen, P.J., Maróti, G., et al. (2021)
800 Pervasive prophage recombination occurs during evolution of spore-forming Bacilli. *ISME J* **15**:
801 1344–1358.

802 Durfee, T., Nelson, R., Baldwin, S., Plunkett, G., Burland, V., Mau, B., et al. (2008) The complete
803 genome sequence of *Escherichia coli* DH10B: insights into the biology of a laboratory
804 workhorse. *J Bacteriol* **190**: 2597–606.

805 Earl, A.M., Losick, R., and Kolter, R. (2008) Ecology and genomics of *Bacillus subtilis*. *Trends*
806 *Microbiol* **16**: 269–275.

807 Eichenberger, P., Fujita, M., Jensen, S.T., Conlon, E.M., Rudner, D.Z., Wang, S.T., et al. (2004) The
808 program of gene transcription for a single differentiating cell type during sporulation in *Bacillus*
809 *subtilis*. *PLoS Biol* **2**: e328.

Erez, Z., Steinberger-Levy, I., Shamir, M., Doron, S., Stokar-Avihail, A., Peleg, Y., et al. (2017) Communication between viruses guides lysis–lysogeny decisions. *Nature* **541**: 488–493.

Fan, B., Blom, J., Klenk, H.P., and Borriss, R. (2017) *Bacillus amyloliquefaciens*, *Bacillus velezensis*, and *Bacillus siamensis* Form an "Operational Group *B. amyloliquefaciens*" within the *B. subtilis* species complex. *Front Microbiol* **8**: 1–15.

Fan, N., Cutting, S., and Losick, R. (1992) Characterization of the *Bacillus subtilis* sporulation gene *spoVK*. *J Bacteriol* **174**: 1053–4.

FERNANDES, R.M., DE LENCASTRE, H., and ARCHER, L.J. (1986) Three New Temperate Phages of *Bacillus subtilis*. *Microbiology* **132**: 661–668.

Feucht, A., Evans, L., and Errington, J. (2003) Identification of sporulation genes by genome-wide analysis of the σ E regulon of *Bacillus subtilis*. *Microbiology* **149**: 3023–3034.

Fink, P.S. and Zahler, S.A. (1982) Restriction fragment maps of the genome of *Bacillus subtilis* bacteriophage SPβ. *Gene* **19**: 235–238.

Forrest, D., James, K., Yuzenkova, Y., and Zenkin, N. (2017) Single-peptide DNA-dependent RNA polymerase homologous to multi-subunit RNA polymerase. *Nat Commun* **8**: 1–8.

Fritze, D. (2004) Taxonomy of the Genus *Bacillus* and Related Genera: The Aerobic Endospore-Forming Bacteria. *Phytopathology* **94**: 1245–8.

Gallego Del Sol, F., Penadés, J.R., and Marina, A. (2019) Deciphering the Molecular Mechanism Underpinning Phage Arbitrium Communication Systems. *Mol Cell* **74**: 59-72.e3.

Gruber, A.R., Lorenz, R., Bernhart, S.H., Neuböck, R., and Hofacker, I.L. (2008) The Vienna RNA websuite. *Nucleic Acids Res* **36**: W70-4.

Hemphill, H.E., Gage, I., Zahler, S.A., and Korman, R.Z. (1980) Prophage-mediated production of a bacteriocinlike substance by SPβ lysogens of *Bacillus subtilis*. *Can J Microbiol* **26**: 1328–1333.

Hemphill, H.E. and Whiteley, H.R. (1975) Bacteriophages of *Bacillus subtilis*. *Bacteriol Rev* **39**: 257–315.

Holberger, L.E., Garza-Sánchez, F., Lamoureux, J., Low, D.A., and Hayes, C.S. (2012) A novel family of toxin/antitoxin proteins in *Bacillus* species. *FEBS Lett* **586**: 132–136.

Johnson, C.M. and Grossman, A.D. (2016) Complete Genome Sequence of *Bacillus subtilis* Strain CU1050, Which Is Sensitive to Phage SPβ. *Genome Announc* **4**: e00262-16.

Jones, P., Binns, D., Chang, H.-Y., Fraser, M., Li, W., McAnulla, C., et al. (2014) InterProScan 5: genome-scale protein function classification. *Bioinformatics* **30**: 1236–1240.

Klumpp, J., Lavigne, R., Loessner, M.J., and Ackermann, H.W. (2010) The SPO1-related bacteriophages. *Arch Virol* **155**: 1547–1561.

Kohm, K., Basu, S., Nawaz, M.M., and Hertel, R. (2021) Chances and limitations when uncovering essential and non-essential genes of *Bacillus subtilis* phages with CRISPR-Cas9. *Environ Microbiol Rep* **accepted**: 1758-2229.13005.

Kohm, K. and Hertel, R. (2021) The life cycle of SPβ and related phages. *Arch Virol* **166**: 2119–2130.

Koo, B., Kritikos, G., Farelli, J.D., Todor, H., Tong, K., Kimsey, H., et al. (2017) Construction and Analysis of Two Genome-Scale Deletion Libraries for *Bacillus subtilis*. *Cell Syst* **4**: 291-305.e7.

Kunst, F., Ogasawara, N., Moszer, I., Albertini, A.M., Alloni, G., Azevedo, V., et al. (1997) The complete genome sequence of the gram-positive bacterium *Bacillus subtilis*. *Nature* **390**: 249–56.

852 Langmead, B. and Salzberg, S.L. (2012) Fast gapped-read alignment with Bowtie 2. *Nat Methods* **9**:
853 357–359.

854 Lazarevic, V., Düsterhöft, A., Soldo, B., Hilbert, H., Mauël, C., and Karamata, D. (1999) Nucleotide
855 sequence of the *Bacillus subtilis* temperate bacteriophage SPβc2. *Microbiology* **145 (Pt 5**: 1055–
856 1067.

857 Lechner, M., Findeiß, S., Steiner, L., Marz, M., Stadler, P.F., and Prohaska, S.J. (2011) Proteinortho:
858 Detection of (Co-)orthologs in large-scale analysis. *BMC Bioinformatics* **12**: 124.

859 Lee, C.A., Auchtung, J.M., Monson, R.E., and Grossman, A.D. (2007) Identification and
860 characterization of *int* (integrase), *xis* (excisionase) and chromosomal attachment sites of the
861 integrative and conjugative element ICEBs1 of Bacillus subtilis. *Mol Microbiol* **66**: 1356–69.

862 McLaughlin, J.R., Wong, H.C., Ting, Y.E., Van Arsdell, J.N., and Chang, S. (1986) Control of
863 Lysogeny and Immunity of *Bacillus subtilis* Temperate Bacteriophage SPβ by Its d Gene. *J*
864 *Bacteriol* **167**: 952–9.

865 Meijer, W.J.J., Horcajadas, J.A., and Salas, M. (2001) φ29 Family of Phages. *Microbiol Mol Biol Rev*
866 **65**: 261–287.

867 Van Melderen, L. (2010) Toxin–antitoxin systems: why so many, what for? *Curr Opin Microbiol* **13**:
868 781–785.

869 Mi, H., Muruganujan, A., and Thomas, P.D. (2013) PANTHER in 2013: modeling the evolution of
870 gene function, and other gene attributes, in the context of phylogenetic trees. *Nucleic Acids Res*
871 **41**: D377-86.

872 Miller, J.H. (1972) Experiments in molecular genetics, Cold Spring Harbor Laboratory Press,U.S.

873 Milne, I., Bayer, M., Cardle, L., Shaw, P., Stephen, G., Wright, F., and Marshall, D. (2010) Tablet--
874 next generation sequence assembly visualization. *Bioinformatics* **26**: 401–2.

875 Nicolas, P., Mäder, U., Dervyn, E., Rochat, T., Leduc, A., Pigeonneau, N., et al. (2012) Condition-
876 dependent transcriptome reveals high-level regulatory architecture in *Bacillus subtilis*. *Science*
877 **335**: 1103–6.

878 Nordmann, B., Schilling, T., Hoppert, M., and Hertel, R. (2019) Complete genome sequence of the
879 virus isolate vB_BthM-Goe5 infecting *Bacillus thuringiensis*. *Arch Virol* **164**: 1485–1488.

880 Noyer-Weidner, M., Jentsch, S., Pawlek, B., Günthert, U., and Trautner, T.A. (1983) Restriction and
881 modification in *Bacillus subtilis*: DNA methylation potential of the related bacteriophages Z,
882 SPR, SPβ, φ3T, and ρ11. *J Virol* **46**: 446–453.

883 Otte, K., Kühne, N.M., Furrer, A.D., Baena Lozada, L.P., Lutz, V.T., Schilling, T., and Hertel, R.
884 (2020) A CRISPR-Cas9 tool to explore the genetics of *Bacillus subtilis* phages. *Lett Appl*
885 *Microbiol* **71**: 588–595.

886 Popp, P.F., Benjdia, A., Strahl, H., Berteau, O., and Mascher, T. (2020) The Epipeptide YydF
887 Intrinsically Triggers the Cell Envelope Stress Response of *Bacillus subtilis* and Causes Severe
888 Membrane Perturbations. *Front Microbiol* **11**: 151.

889 Regamey, A. and Karamata, D. (1998) The n-acetylmuramoyl-l-alanine amidase encoded by the
890 *Bacillus subtilis* 168 prophage SPβ. *Microbiology* **144**: 885–893.

891 Reilly, B.E. and Spizizen, J. (1965) Bacteriophage Deoxyribonucleate Infection of Competent *Bacillus*
892 *subtilis*. *J Bacteriol* **89**: 782–790.

893 Rooney, A.P., Price, N.P.J., Ehrhardt, C., Swezey, J.L., and Bannan, J.D. (2009) Phylogeny and
894 molecular taxonomy of the *Bacillus subtilis* species complex and description of *Bacillus subtilis*

subsp. *inaquosorum* subsp. nov. *Int J Syst Evol Microbiol* **59**: 2429–36.

Sambrook, J. and Russell, D.W. (2001) Molecular cloning : a laboratory manual, Cold Spring Harbor Laboratory Press.

Schilling, T., Dietrich, S., Hoppert, M., and Hertel, R. (2018) A CRISPR-Cas9-Based Toolkit for Fast and Precise In Vivo Genetic Engineering of *Bacillus subtilis* Phages. *Viruses* **10**: 241.

Seaman, E., Tarmy, E., and Marmur, J. (1964) Inducible Phages of *Bacillus subtilis*. *Biochemistry* **3**: 607–613.

Seemann, T. (2014) Prokka: rapid prokaryotic genome annotation. *Bioinformatics* **30**: 2068–2069.

Sonenshein, A.L., Hoch, J.A., and Losick, R. eds. (2001) *Bacillus subtilis* and Its Closest Relatives, Washington, DC, USA: ASM Press.

Spancake, G.A. and Hemphill, H.E. (1985) Deletion Mutants of *Bacillus subtilis* Bacteriophage SPβ. *J Virol* **55**: 39–44.

Spizizen, J. (1958) TRANSFORMATION OF BIOCHEMICALLY DEFICIENT STRAINS OF BACILLUS SUBTILIS BY DEOXYRIBONUCLEATE. *Proc Natl Acad Sci U S A* **44**: 1072–8.

Steil, L., Serrano, M., Henriques, A.O., and Völker, U. (2005) Genome-wide analysis of temporally regulated and compartment-specific gene expression in sporulating cells of *Bacillus subtilis*. *Microbiology* **151**: 399–420.

Suzuki, S., Yoshikawa, M., Imamura, D., Abe, K., Eichenberger, P., and Sato, T. (2020) Compatibility of Site-Specific Recombination Units between Mobile Genetic Elements. *iScience* **23**: 100805.

Taylor, M.J. and Thorne, C.B. (1963) TRANSDUCTION OF *BACILLUS LICHENIFORMIS* AND *BACILLUS SUBTILIS* BY EACH OF TWO PHAGES1. *J Bacteriol* **86**: 452–461.

Tucker, R.G. (1969) Acquisition of Thymidylate Synthetase Activity by a Thymine-requiring Mutant of *Bacillus subtilis* following Infection by the Temperate Phage φ3. *J Gen Virol* **4**: 489–504.

Warner, F.D., Kitos, G.A., Romano, M.P., and Hemphill, H.E. (1977) Characterization of SPβ: a temperate bacteriophage from *Bacillus subtilis* 168M. *Can J Microbiol* **23**: 45–51.

Westers, H., Dorenbos, R., van Dijl, J.M., Kabel, J., Flanagan, T., Devine, K.M., et al. (2003) Genome engineering reveals large dispensable regions in *Bacillus subtilis*. *Mol Biol Evol* **20**: 2076–90.

Wick, R.R., Judd, L.M., Gorrie, C.L., and Holt, K.E. (2017) Unicycler: Resolving bacterial genome assemblies from short and long sequencing reads. *PLOS Comput Biol* **13**: e1005595.

Willms, I.M., Hoppert, M., and Hertel, R. (2017) Characterization of *Bacillus subtilis* Viruses vB_BsuM-Goe2 and vB_BsuM-Goe3. *Viruses* **9**: 146.

Zahler, S.A., Korman, R.Z., Thomas, C., Fink, P.S., Weiner, M.P., and Odebralski, J.M. (1987) H2, a Temperate Bacteriophage Isolated from *Bacillus amyloliquefaciens* Strain H. *Microbiology* **133**: 2937–2944.

Zahler, S.A., Korman, R.Z., Thomas, C., and Odebralski, J.M. (1987) Temperate Bacteriophages of *Bacillus amylolquefaciens*. *Microbiology* **133**: 2933–2935.

Figures and Tables captions

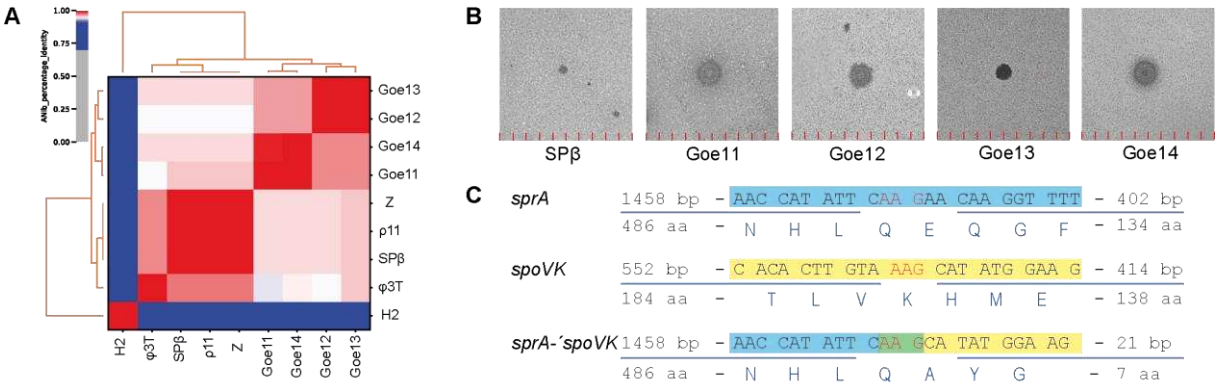

Figure 1: ***A:*** *Whole-genome average nucleotide identity analysis of experimentally verified SPβ-like phages. White to red indicates identity values between 95 to 100 % and thus strains of the same species. White to blue indicates values 95 to 70 % and thus strains of the same genus.* ***B:*** *Plaques of new wild type isolates in comparison to the type strain SPβ. The plaques are presented in one square centimetre section. The red lines are a millimetre scale.* ***C:*** *Goe14 integration into the spoVK gene of B. subtilis. The sprA-like phage integrase, presented in blue, recombines the attP site (AAG) located in its coding sequence with the attB site in the spoVK gene, where those three bases present a triplet coding for lysine. Upon recombination, the sprA-like integrase gene of Goe14 alters its C-terminal coding region. It becomes significantly shorter.*

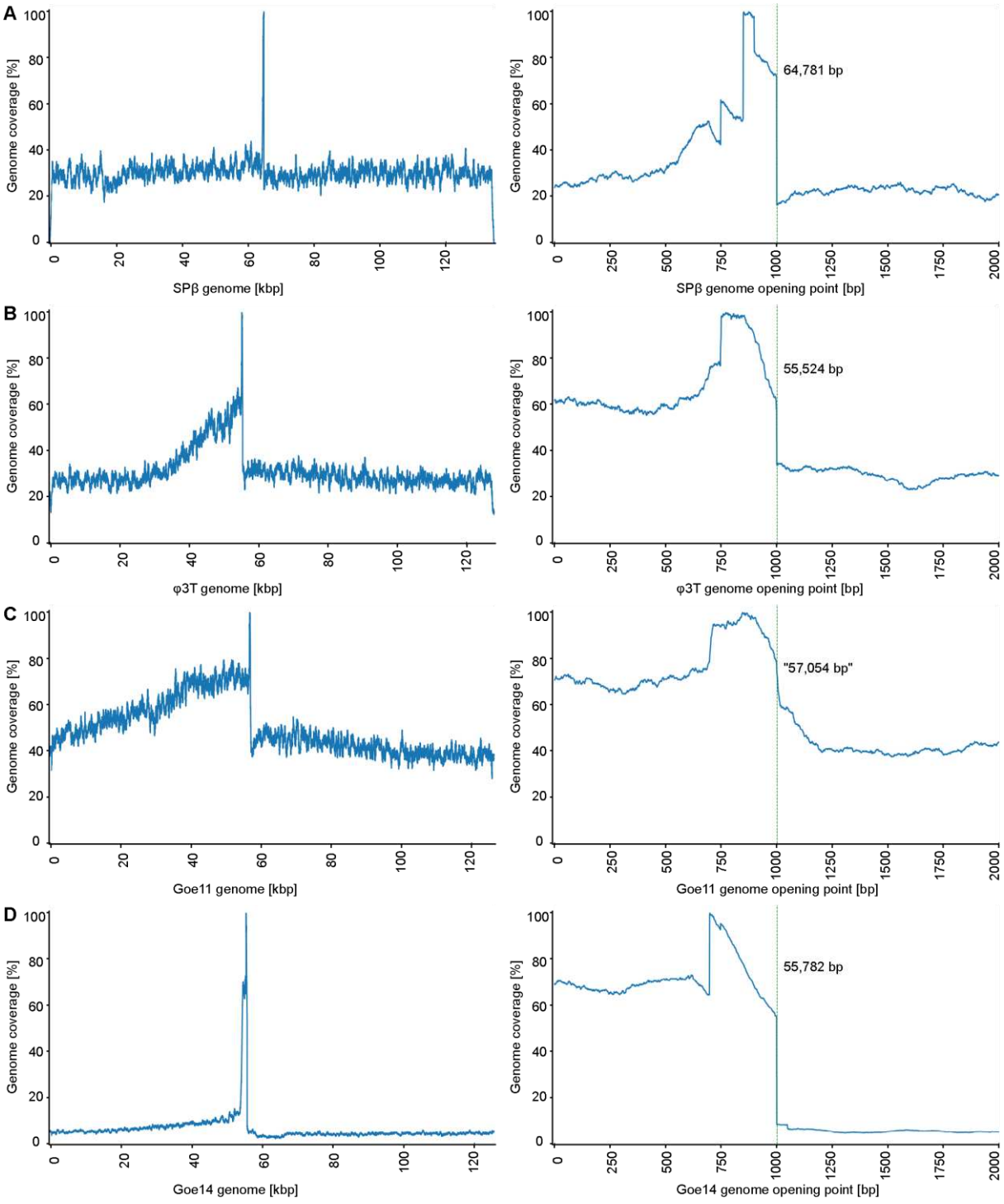

Figure 2: Phage genomes coverage plots. Left panels show the distribution of raw sequence read over the respective phage genome. The counter-clockwise fate out of read coverage from the coverage peak indicates a pac-site as the initiation point of genome packaging and a head-full mechanism of a concatemeric template. The packaging direction corresponds to the read fate out. Right panels present zooms into the coverage peak, which presents the respective genome opening points and the predicted first base packed into the phage head. The predicted opening point of Goe11 is set in quotation marks as we expect it to be slightly imprecise.

Figure 3: Identified integration loci for SPβ-like phage present in B. subtilis 168.

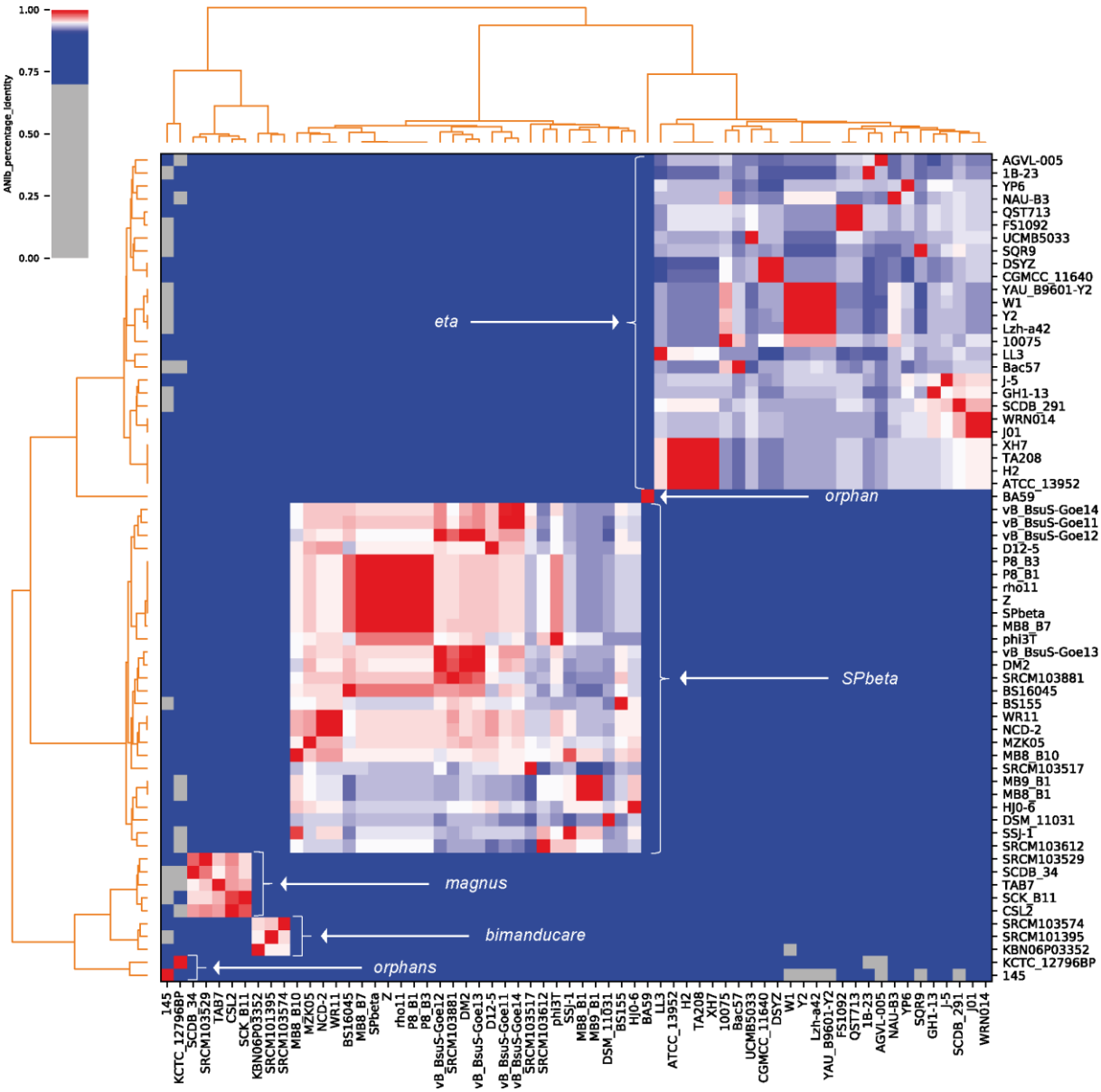

Figure 4: Average nucleotide identity analysis of SPβ-like phages. Analysis reveals seven viral species clusters.

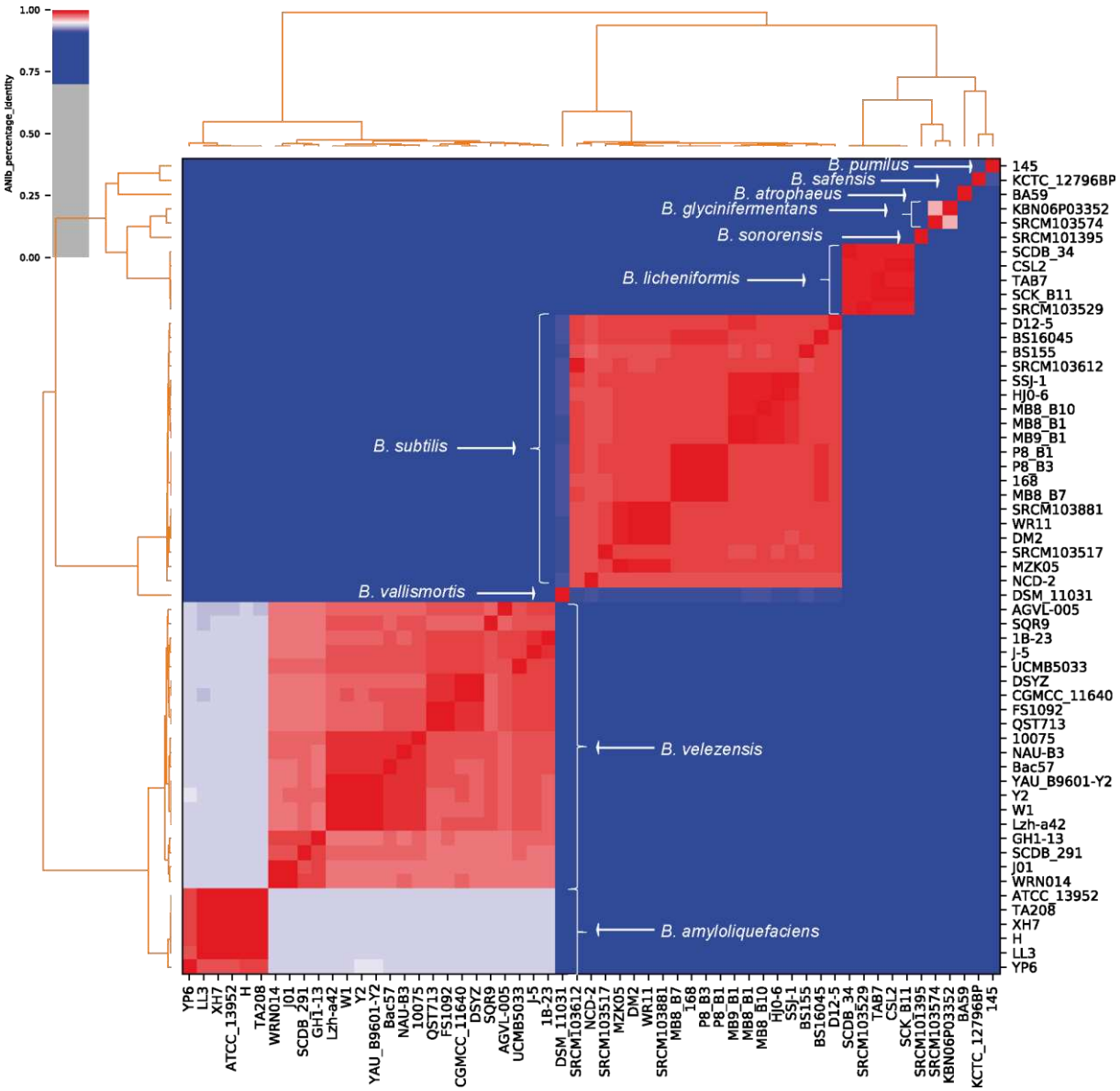

Figure 5: Average nucleotide identity analysis of SPβ-like host strains. Analysis reveals ten host species employed by Spbetavirus.

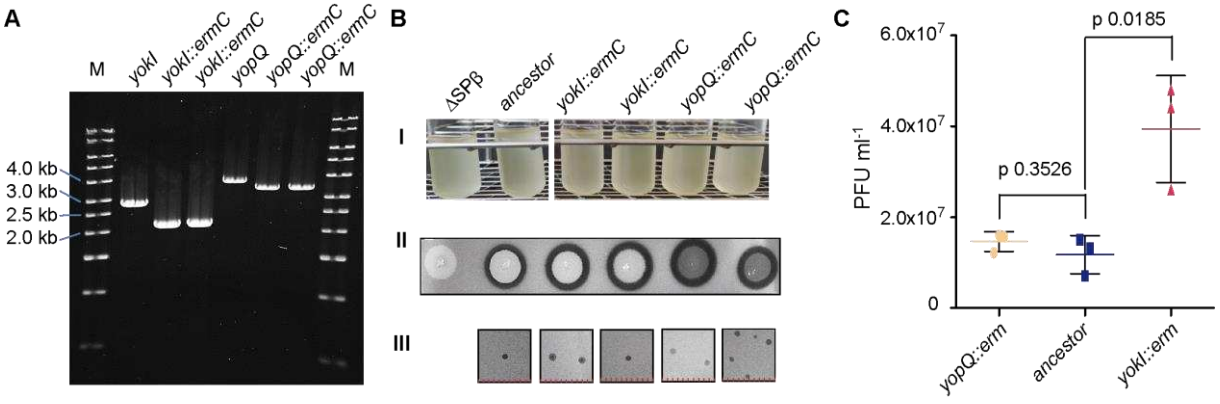

961

962 *Figure 6: Investigation of the yokI, yopQ mutants.* ***A:*** *PCR control of the yokI and yopQ mutants. The primers*
963 *PP342/PP345 were used to amplify the yokI locus and results with the wild type situation in a 2.7 kbp fragment and*
964 *with the mutant in 2.1 kbp. To verify the yopQ locus, the primers PP073/PP319 were used. The wild type situation*
965 *led to a 3.7 kbp fragment and the mutant to 3.5 kbp. All PCR fragments revealed the expected size.* ***B I:*** *Growth*
966 *experiment of all investigated strains in liquid LB medium. No particularities were observed.* ***II.*** *Verification of SPβ*
967 *prophages. Bacteria with an SPβ prophage secret sublancin 168, which is toxic to SPβ free strains. Lysogens*
968 *applied to a layer of an SPβ free sensory strain generate an inhibition zone around themselves and thus verify the*
969 *presence of an SPβ prophage in the tested strain. All tested mutant strains secreted sublancin 168 and thus proved*
970 *the presence of SPβ.* ***III.*** *Verification of phage viability. All investigated mutants released viable virions in the*
971 *supernatant confirmed via plaque formation.* ***C:*** *Release of viable SPβ virions into the supernatant in cultures of*
972 *lysogenic bacteria. The SPβ yokI::ermC mutant releases about four times more virions compared to the ancestor*
973 *strain of the mutant. The p-values were determined by an unpaired t-test. Horizontal bars indicate the respective*
974 *mean values. Error bars indicate standard deviation.*

975

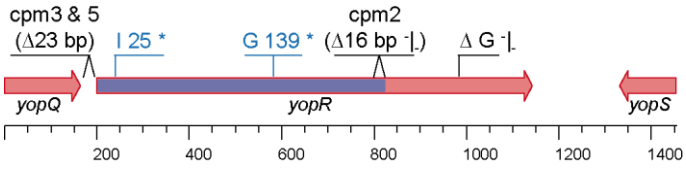

976

977 *Figure 7: Mutation analysis of yopR clear plaque mutants (cpm). Mutations indicated in black were discovered*
978 *during the presented study. Mutations presented in blue were discovered by Brady et. al.* (Brady *et al.*, 2021)*. The*
979 *bar in the yopR gene marks the predicted DNA breaking-rejoining catalytic core domain. * = stop codon. ⁻|.* =
980 frameshift.

981

982

983

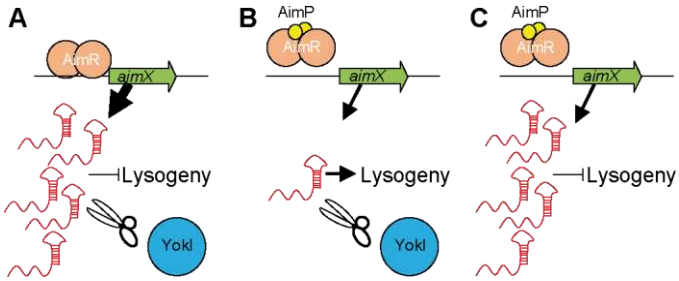

Figure 8: The hypothetical role of YokI as AimX concentration balancer. ***A:*** *Early infection situation. AimR binds to the aimX promoter and activates transcription of the ncRNA AimX, which in turn represses lysogeny. YokI degrades the constantly transcribed AimX and avoids AimX accumulation.* ***B:*** *Late infection situation. The signal peptide AimP binds to AimR, the complex dissociates from the aimX promoter and AimX transcription is reduced, YokI degrades the remaining AimX what activates lysogeny.* ***C:*** *Late infection situation in deletion yokI mutant. The signal peptide AimP binds to AimR, the complex dissociates from the aimX promoter reducing AimX transcription. However, in the absence of YokI, present AimX is not degraded, accumulates, and reduces lysogeny.*

Table 1: New SPβ-like phages

Proposed species	Phage strain	Host	*attP* sequence 5'->3'	*attB* sequence 5'->3'	Integration locus	Phage genome in bp	Accesion number	Prophage position	Ref.
SPbeta	SPβ	*B. subtilis* 168	**ACAG**AT*AA*/A**GCTGT**AT	**ACAG**AT*AA*/A**GCTGT**AT	*spsM*	134402	NC_000964	2152031..2286432	
	Z	*B. subtilis* CU1065	**ACAG**AT*AA*/A**GCTGT**AT	**ACAG**AT*AA*/A**GCTGT**AT	*spsM*	134402	NZ_JADOXU010000001	Contig 5, 19, 2	
	ρ11	*B. subtilis* DBS-15	**ACAG**AT*AA*/A**GCTGT**AT	**ACAG**AT*AA*/A**GCTGT**AT	*spsM*	134402	JADOXP010000001	Contig 6, 16, 3	
	Goe12	*B. subtilis* Δ6	**ACAG**AT*AA*/A**GCTGT**AT*	**ACAG**AT*AA*/A**GCTGT**AT	*spsM*	124287	MT601273	n.d.	
	Goe13	*B. subtilis* Δ6	**ACAG**AT*AA*/A**GCTGT**AT*	**ACAG**AT*AA*/A**GCTGT**AT	*spsM*	126848	MT601274	n.d.	
	NCD-2	*B. subtilis* NCD-2	**ACAG**AT*AA*/A**GCTGT**AT	**ACAG**AT*AA*/A**GCTGT**AT	*spsM*	130585	CP023755	2120469..2251053	
	WR11	*Bacillus sp.* WR11	**ACAG**AT*AA*/A**GCTGT**AT	**ACAG**AT*AA*/A**GCTGT**AT	*spsM*	130597	CP033064	2116505..2247101	
	DM2	*Bacillus sp.* DM2	**ACAG**AT*AA*/A**GCaGT**AT	**ACAG**AT*AA*/A**GCTGT**AT	*spsM*	122713	CP030937	2164120..2286832	
	SRCM103517	*B. subtilis* SRCM103517	**ACAG**AT*AA*/A**GCTGTt**T	**ACAG**AT*AA*/A**GCTGT**AT	*spsM*	134921	CP035226	2174195..2309115	
	SRCM103881	*B. subtilis* SRCM103881	**ACAG**AT*AA*/A**GCTGT**AT	**ACAG**AT*AA*/A**GCTGT**AT	*spsM*	123645	CP035165	2116561..2240175	
	SRCM103612	*B. subtilis* SRCM103612	**ACAG**AT*AA*/A**GCTGT**AT	**ACAG**AT*AA*/A**GCTGT**AT	*spsM*	129386	CP035406	2104311..2233696	
	P8_B3	*B. subtilis* P8_B3	**ACAG**AT*AA*/A**GCTGT**AT	**ACAG**AT*AA*/A**GCTGT**AT	*spsM*	134403	NZ_CP045812	2151638..2286040	
	P8_B1	*B. subtilis* P8_B1	**ACAG**AT*AA*/A**GCTGT**AT	**ACAG**AT*AA*/A**GCTGT**AT	*spsM*	134403	NZ_CP045922	2151638..2286040	
	MB9_B1	*B. subtilis* MB9_B1	**ACAG**AT*AA*/A**GCTGT**AT	**ACAG**AT*AA*/A**GCTGT**AT	*spsM*	135871	NZ_CP045820	2179740..2315610	
	MB8_B7	*B. subtilis* MB8_B7	**ACAG**AT*AA*/A**GCTGT**AT	**ACAG**AT*AA*/A**GCTGT**AT	*spsM*	136192	NZ_CP045821	2131132..2267323	
	MB8_B1	*B. subtilis* MB8_B1	**ACAG**AT*AA*/A**GCTGT**AT	**ACAG**AT*AA*/A**GCTGT**AT	*spsM*	135871	NZ_CP045823	2137059..2272929	
	MB8_B10	*B. subtilis* MB8_B10	aaaacgacataCCTACtgtgttttt	gctatgcggttCCTACctttgtcgtt	*kamA*	134854	NZ_CP045824	2136840..2271693	
	BS16045	*B. subtilis* BS16045	aaaatgacataCCTACtgtgttttt	gctatgcggttCCTACctttgtcgtt	*kamA*	128860	NZ_CP017112	2117777..2246636	
	D12-5	*B. subtilis* D12-5	aaaacgacataCCTACtgtgttttt	gctatgcggttCCTACctttgtcgtt	*kamA*	131142	CP014858	1898529..2029670	
	Goe11	*B. subtilis* Δ6	aaaatgacataCCTACtgtgttttt*	gctatgcggttCCTACctttgtcgtt	*kamA*	126288	MT601272	n.d.	
	φ3T	*B. subtilis* 168	aaaatgacataCCTACtgtgttttta	gctatgcggttCCTACctttgtcgtt	*kamA*	128375	KY030782	n.d.	(Erez *et al.*, 2017)
	Goe14	*B. subtilis* Δ6	aaccatattcAAGaacaaggttt	cacacttgtaAAGcatatggaag	*spoVK*	125490	OL580764	n.d.	
	SSJ-1	*B. subtilis* SSJ-1	aaccatattcAAGaacaagttt	tttgggaaagAAGcgatcgacac	*spoVK*	129917	NZ_CP032860	3384159..3514075	
	BS155	*B. subtilis* BS155	aaccatattcAAGaacaagttt	cacacttgtaAAGcatatggaag	*spoVK*	121708	CP029052	1953540..2075247	
	HJ0-6	*B. subtilis* HJ0-6	aaccatattcAAGaacaagttt	cacacttgtcAAGcatatggaag	*spoVK*	121686	CP016894	1827893..1949578	
	MZK05	*B. subtilis* MZK05	aaccatattcAAGaacaagttt	cacacttgtcAAGcatatggaag	*spoVK*	128800	NZ_CP032315	1786644..19115443	
	DSM 11031	*B. vallismortis* DSM 11031	aactatgttcAAGaacaagttt	cacgctcgtcAAGcatatggaag	*spoVK*	134142	CP026362	1564098..1698239	
eta	SCDB 291	*B. velezensis* SCDB 291	ctttgccgtgCCTACctttgtcgtc	aaacaatgtgCCGACagcatttttt	*kamA*	134787	CP022654	4160999..133216	
	SQR9	*B. velezensis* SQR9	aaatgctgtaGGCACattgttttt	gacaaaggtcGGCACggcaaagccc	*kamA*	136026	NZ_CP006890	2132735..2268760	
	10075	*B. velezensis* 10075	aaccgttattcAAGaacaagttt	tacgcttgtcAAGcatatggaag	*spoVK*	122481	NZ_CP025939	1413915..1536395	
	Bac57	*B. velezensis* Bac57	aaccgttattcAAGaacaagttt	tacgcttgtcAAGcatatggaag	*spoVK*	139215	NZ_CP033054	2108355..2247569	
	GH1-13	*B. velezensis* GH1-13	aaccgttattcAAGaacaagttt	tacgcttgtcAAAcatatggaag	*spoVK*	139040	NZ_CP019040	1805602..1945196	
	1B-23	*B. velezensis* 1B-23	ATAATtcTTACgA	ATAATcgTCACaA	*pbuX*	135793	CP033967	2452301..2588093	
	J01	*B. velezensis* J01	ATAATtcTTACgA	ATAATcgTCACaA	*pbuX*	134525	NZ_CP023133	1693622..1828146	
	AGVL-005	*B. velezensis* AGVL-005	ATAATtcTTACgA	ATAATcgTCACaA	*pbuX*	134737	CP024922	2313534..2178798	
	QST713	*B. velezensis* QST713	ATAActcTTACgA	ATAATcgTCACaA	*pbuX*	135374	NZ_CP025079	2328962..2193589	
	CGMCC 11640	*B. velezensis* CGMCC 11640	ATAATCGTtACgA	ATAATCGTcACaA	*pbuX*	138554	NZ_CP026610	2289554..2428107	
	DSYZ	*B. velezensis* DSYZ	ATAATCGTtACgA	ATAATCGTcACaA	*pbuX*	138582	NZ_CP030150	2289275..2427856	
	WRN014	*B. velezensis* WRN014	ATAATtcTTACgA	ATAATCGTcACaA	*pbuX*	134525	CP041361	2182837..2317361	
	NAU-B3	*B. velezensis* NAU-B3	GTGACGATTATGGAT	GTGACGATTATcgGGAT	*pbuX*	137778	NC_022530	1644861..1782638	
	UCMB5033	*B. velezensis* UCMB5033	ATAATtcTtACgA	ATAATCGTcACaA	*pbuX*	138610	NC_022075	2150738..2289347	
	ATCC 13952	***B. subtilis* ATCC 13952*[1]**	ATAATtcTTACAA	ATAATcgTTACAA	*pbuX*	134868	NZ_CP009748	2062692..2197559	
	J-5	***B. subtilis* J-5*[1]**	ATAATtcTTACgA	ATAATcgTTACAA	*pbuX*	135839	NZ_CP018295	2203185..2339023	
	Lzh-a42	*B. velezensis* Lzh-a42	GATATGTTCCGCACACAGGTTCATCC GTGGGAGCGCGAACAaTAcATGTCTC AGTATTAATCTCTCAATCCCTTGGCA CTATTGGTGTCAGGGGATTTTTTGGT TT	GATATGTTCCGCACACAGGTTCATCC GTGGGAGCGCGAACAgTAtATGTCTC AGTATTAATCTCTCAATCCCTTGGCA CTATTGGTGTCAGGGGATTTTTTGGT TT	*glnA*	137347	NZ_CP025308	1837732..1975078	
	W1	*B. velezensis* W1	GATATGTTCCGCACACAGGTTCATCC GTGGGAGCGCGAACAaTAcATGTCTC AGTATTAATCTCTCAATCCCTTGGCA CTATTGGTGTCAGGGGATTTTTTGGT TT	GATATGTTCCGCACACAGGTTCATCC GTGGGAGCGCGAACAgTAtATGTCTC AGTATTAATCTCTCAATCCCTTGGCA CTATTGGTGTCAGGGGATTTTTTGGT TT	*glnA*	137359	CP028375	1855846..1993204	
	YAU B9601-Y2	*B. velezensis* YAU B9601-Y2	GATATGTTCCGCACACAGGTTCATCC GTGGGAGCGCGAACAaTAcATGTCTC AGTATTAATCTCTCAATCCCTTGGCA CTATTGGTGTCAGGGGATTTTTTGGT TT	GATATGTTCCGCACACAGGTTCATCC GTGGGAGCGCGAACAgTAtATGTCTC AGTATTAATCTCTCAATCCCTTGGCA CTATTGGTGTCAGGGGATTTTTTGGT TT	*glnA*	137349	NC_017061	1862073..1999421	
	H2	*B. amyloliquefaciens* H	ATAATtcTTACAA	ATAATcgTTACAA	*pbuX*	134868	CP041693	1974393..2109260	(Zahler, Korman, Thomas, and Odebralski, 1987)
	YP6	*B. amyloliquefaciens* YP6	ATtATaGTttaAg	ATaATcGTcacAa	*pbuX*	141939	CP032146	2122388..2264326	
	FS1092	*B. amyloliquefaciens* FS1092	ATAActcTTACgA	ATAATCGTcACaA	*pbuX*	136328	CP038028	3773157..3909484	
	LL3	*B. amyloliquefaciens* LL3	ATAATTCTTACAA	ATAATCGTTACAA	*pbuX*	139754	NC_017190	2139580..2279333	
	TA208	*B. amyloliquefaciens* TA208	ATAATTCTTACAA	ATAATCGTTACAA	*pbuX*	134868	NC_017188	1178154..1313021	
	XH7	*B. amyloliquefaciens* XH7	ATAATTCTTACAA	ATAATCGTTACAA	*pbuX*	134868	NC_017191	1179731..1314598	
	Y2	***B. amyloliquefaciens* Y2*[2]**	GATATGTTCCGCACACAGGTTCATCC GTGGGAGCGCGAACAaTAcATGTCTC AGTATTAATCTCTCAATCCCTTGGCA CTATTGGTGTCAGGGGATTTTTTGGT TT	GATATGTTCCGCACACAGGTTCATCC GTGGGAGCGCGAACAgTAtATGTCTC AGTATTAATCTCTCAATCCCTTGGCA CTATTGGTGTCAGGGGATTTTTTGGT TT	*glnA*	137350	NC_017912	1858198..1995547	
magnus	TAB7	*B. licheniformis* TAB7	aaacgcagtaGGgacagtgttt	gacaaaggtcGGcactgcatag	*kamA*	145790	CP027789	2241119..2386908	
	SRCM103529	*B. licheniformis* SRCM103529	aaacgcagtaGGgacagtgttt	gacaaaggtcGGcactgcatag	*kamA*	146820	CP035228	2318400..2465381	
	SCDB 34	*B. licheniformis* SCDB 34	taaactatgtTCAAgaACaaggtttaa	gatacattggTCAAACatatggagga	*spoVK*	145801	CP014793	324753..469729	
	CSL2	*B. licheniformis* CSL2	taaactatgtTCAAgaACaaggtttaa	gatacattggTCAAACatatggagga	*spoVK*	139312	CP041154	1900772..2040083	
	SCK B11	*B. licheniformis* SCK B11	taaactatgtTCAAgaACaaggtttaa	gatacattggTCAAACatatggagga	*spoVK*	135335	NZ_CP014795	499..135833	
bimanducare	KBN06P03352	*B. glycinifermentans* KBN06P03352	aaccatattcAAGaacatggttt	cacattagtaAAAcatatggaag	*spoVK*	136407	CP023481	442875..579281	
	SRCM103574	*B. glycinifermentans* SRCM103574	atataaaactGACTCgtctgtcatt	cgcgatgacgGACTCtccggtatta	*spoVFB*	142121	CP035232	1908002..20500092	
	SRCM101395	*B. sonorensis* SRCM101395	aaccatattcAAGaacatggttt	cacattggtaAAAcatatggaag	*spoVK*	141302	NZ_CP021920	2540170..2681471	
	BA59	*B. atrophaeus* BA59	aaccatattcAAGaacaggttt	cacgctcgtaAAGcatatggaag	*spoVK*	132289	CP024051	2588833..2721121	
	KCTC 12796BP	*B. safensis* KCTC 12796BP	gaccttattcAAGaacatagttt	tacccttgtaAAAcatatggagg	*spoVK*	128597	NZ_CP018197	1697505..1826101	
	145	*B. pumilus* 145	aataccgcttACGACAGAtatagttttgg	aataatggtgACGACAGAccctgtcacg	*pbuX*	129749	CP027116	2018888..2148636	

*[*1] Genome identity analysis revealed the B. subtilis strains to be B. velezensis strains and [*2] B. amyloliquefaciens Y2 to be also B. velezensis. Capital letters at attP/B sites present the direct repeat, which results from prophage integration. Lowercase letters inside an attP/B site indicate variations. Surrounding lowercase letters are presented in cases of very short attP/B repeats. The attP/B sites associated with the spsM gene are presented as described for SPβ* (Abe *et al.*, 2017).

996 Table 2: Core protein genes of the genus *Spbetavirus*

Locus tag	Gene	Annotation	Present in	Cluster
BSU_19830	*yotM*	hypothetical protein	all	II (early genes)
BSU_19990	*yosV*	hypothetical protein	-2	
BSU_20040	*nrdF (yosP)*	ribonucleoside diphosphate reductase	all	
BSU_20060	*yosN*	ribonucleoside reductase alpha subunit	all	
BSU_20070	*nrdIB (yosM)*	putative subunit of nucleoside diphosphate reductase	all	
BSU_20080	*yosL*	hypothetical protein	-1	
BSU_20290	*yorQ*	hypothetical protein	all	
BSU_20330	*yorM*	hypothetical protein	all	
BSU_20360	*yorJ*	putative DNA replication initiation protein	all	
BSU_20410	*yorE*	hypothetical protein	all	
BSU_20480	*yoqX*	hypothetical protein	all	
BSU_20500	*yoqV*	DNA ligase	-2	
BSU_20570	*yoqN*	hypothetical protein	-2	
BSU_20750	*ligB (yopV)*	hypothetical protein	all	
BSU_20790	*yopR*	putative DNA breaking-rejoining enzyme	all	
BSU_20800	*yopQ*	hypothetical protein	all	
BSU_20810	*yopP*	putative phage integrase	all	
BSU_20860	*aimR (yopK)*	arbitrium transcription regulator	all	
BSU_20980	*yonV*	hypothetical protein	-1	III (late genes)
BSU_21040	*yonO*	DNA-dependent RNA polymerase	all	
BSU_21050	*hupN (yonN)*	putative HU-related DNA-binding protein	-2	
BSU_21070	*yonJ*	hypothetical protein	-1	
BSU_21120	*yonE*	hypothetical protein	all	
BSU_21190	*yomX*	hypothetical protein	all	
BSU_21200	*yomW*	hypothetical protein	-1	
BSU_21210	*yomV*	hypothetical protein	all	
BSU_21220	*yomU*	hypothetical protein	all	
BSU_21240	*yomS*	putative phage-related lytic exoenzyme	all	
BSU_21250	*yomR*	hypothetical protein	all	
BSU_21280	*yomO*	hypothetical protein	-1	
BSU_21290	*yomN*	hypothetical protein	all	
BSU_21300	*yomM*	putative integrase	all	
BSU_21350	*cwlP (yomI)*	lytic transglycosylase	all	
BSU_21360	*yomH*	hypothetical protein	-1	
BSU_21370	*yomG*	putative DNA wielding protein	-1	
BSU_21380	*yomF*	hypothetical protein	-1	
BSU_21410	*blyA*	N-acetylmuramoyl-L-alanine amidase	-1	
BSU_21580	*yokI*	putative RNase	all	I (early genes)

997 *Locus tags of genes presented in bold were identified as transcriptionally active on the prophage in microarray experiments*
998 (Nicolas *et al.*, 2012). *Underlined locus tags were identified as transcriptionally active on the prophage in RNA-seq*
999 *experiments* (Popp *et al.*, 2020; Benda *et al.*, 2021).

1000